KYAMBOGO UNIVERSITY

FACULTY OF ENGINEERING

DEPARTMENT OF CIVIL AND BUILDING ENGINEERING

ASSESSING IMPACTS OF CLIMATE CHANGE ON HYDROLOGICAL EXTREMES OF RWIZI CATCHMENT

BY

BARAZA GERALD

(BSc. Agricultural Mechanization & Irrigation Engineering)

REG. NO: 17/U/14672/GMEW/PE

A RESEARCH THESIS SUBMITTED TO KYAMBOGO UNIVERSITY GRADUATE SCHOOL IN PARTIAL FULFILMENT OF THE REQUIREMENTS FOR THE AWARD OF MASTER OF SCIENCE IN WATER AND SANITATION ENGINEERING DEGREE OF KYAMBOGO UNIVERSITY

NOVEMBER, 2019

APPROVAL

The undersigned approve that they have read and hereby recommend for submission to Kyambogo University a dissertation entitled: ASSESSING IMPACTS OF CLIMATE CHANGE ON HYDROLOGICAL EXTREMES OF RWIZI CATCHMENT, in partial fulfilment of the requirements for the award of MASTER OF SCIENCE IN WATER AND SANITATION ENGINEERING degree of Kyambogo University.

Sign: …….

Dr Charles Onyutha (Main Supervisor)

Date:

Sign: …….

Dr Kenan Okurut (Co-Supervisor)

Date:

DECLARATION

I, Gerald Baraza, hereby declare that this submission is my own work and that, to the best of my knowledge and belief, it contains no material previously published or written by another person nor material which has been accepted for the award of any other degree of the university or other institute of higher learning, except where due acknowledgement has been made in the text and reference list.

Sign…….

Gerald Baraza

Date:

ACKNOWLEDGEMENTS

I would like to extend my sincere gratitude and appreciation to the following persons who, in contributed towards the completion of this study. My main supervisor Dr. Charles Onyutha for the support, criticism and help he offered to me from start to the end of this study. I cannot forget my Co-Supervisor Dr. Kenan Okurut who at the same time worked closely with Dr Charles Onyutha in guiding me professionally. May your sacrifice be blessed.

With great regard, to my workmates at W&S Consult for always giving me the environment to have my study fit in my daily work.

On this long road to conclusion, I cannot forget my fellow coursemates Catherine, Arnold, Johnson, Deo, Carolyn and Grace whose contribution kept me steadfastly committed. And of course, finally without further ado I would like to applaud myself for the hard work I put in and keeping my focus on check.

Above all, the Almighty God who has been the craftsman behind every air I breathed for giving me the grace to live and do my research successfully.

DEDICATION

This dissertation is dedicated to my mother Ms Jocelyn Kyobuntungi and my brothers Denis and Bruce.

TABLE OF CONTENTS

APPROVAL ..... **i**

DECLARATION ..... **iii**

ACKNOWLEDGEMENTS ..... **iv**

DEDICATION ..... **v**

LIST OF TABLES ..... **ix**

LIST OF FIGURES ..... **x**

LIST OF ACRONYMS ..... **xi**

ABSTRACT ..... **xiii**

CHAPTER ONE: INTROCUCTION **1**

1.1 Background of the Study 1

1.2 Statement of the Problem 4

1.3 Objectives of the Study 5

1.3.1 Main Objective 5

1.3.2 Specific Objectives 5

1.4 Research Questions 5

1.5 Research Justification 5

1.6 Significance of the study 6

1.7 Scope of the Study 6

1.8 Conceptual framework 7

CHAPTER TWO: LITERATURE REVIEW **8**

2.1 Climate of Uganda 8

2.1.1 Past studies on impacts of climate change on water resources in Uganda 8

2.2 Hydrology of River Rwizi Catchment 9

2.3.1 Trend Magnitude 10

2.3.2 Trend direction 11

2.3.3 Past studies on time series analysis 11
2.4 Global Circulation Models (GCMs) 12
2.4.1 Downscaling of GCMs 12
2.4.2 Performance of GCMs in Rwizi Catchment 14
2.5 Selection of scenarios 15
2.7 Hydrological modelling for climate change impact investigation 18
2.7.1 Lumped conceptual modelling for climate change impact investigation .. 19
2.7.2 Lumped conceptual models 19
2.7.3 Calibration of the conceptual models 26
2.7.4 Validation of the conceptual models 27
2.8 Climate change impact investigation on streamflow 27
CHAPTER THREE: MATERIALS AND METHODS 29
3.1 Introduction 29
3.1.1 Study area 29
3.2 Data 31
3.2.1 Rainfall data 31
3.2.2 Observed flow data 32
3.2.3 Potential Evapotranspiration (PET) 32
3.2.4 Downscaled climate data 34
3.3 Time series analysis 34
3.3.1 Trend magnitude 34
3.3.3 Standardization of trend test statistics Z 36
3.4 Projection of future climate conditions from GCMs outputs 37
3.4.1 Climate scenarios selection 37
3.4.2 Selection of GCMs used in this study. 37
3.4.3 Data for future climatic conditions 39

3.5 Selection of lumped conceptual models used for this study 39
3.5.1 Setting up and Evaluation 40
3.6 Future river flows 40
3.6.1 Analysis of the extent of climate change on river flow 41
CHAPTER FOUR: DISCUSSION AND PRESENTATION OF RESULT 42
4.1 Introduction 42
4.2 Time series analysis 42
4.2.1 Trends in precipitation 42
4.2.2 Trends in Potential Evapotranspiration (PET) 46
4.3 Projected change in future climatic conditions 50
4.3.1 Projected change in precipitation 50
4.3.2 Projected change in temperature 52
4.4 Rainfall runoff model 56
4.4.1 Calibration and validation of AWBM 56
4.4.2 Calibration and validation of HMSV 58
4.5 Future streamflow conditions 60
4.5.1 Extraction of high flows. 60
4.5.2 Extraction of low flow quantiles 64
CHAPTER FIVE: CONCLUSIONS AND RECOMMENDATIONS 68
5.1. Conclusions 68
5.2. Recommendations 70
REFERENCES 71
APPENDICES 82

LIST OF TABLES

Table 3.1: Stations within and around Rwizi catchment..... 32

Table 3.2: Basic information of the GCMs used in this study..... 38

Table 4.1: Optimal parameters of AWBM..... 57

Table 4.2: Optimal parameters of HMSV..... 58

LIST OF FIGURES

Figure 1-1: Conceptual framework of the study 7

Figure 2-1: Illustration of developing downscaled climate projections 13

Figure 2-2: AWBM model structure (Source: Boughton, 2004) 21

Figure 2-3: TANK model structure (Source: Podger, 2004) 22

Figure 2-4: Structure of the SMAR model (Source: O'Connell et al., 1970) 24

Figure 2-5: Structure of the SIMHYD model (Source: Porter, 1972) 25

Figure 2-6: Schematic representation of HMSV (Source: Onyutha, 2019) 26

Figure 3-1: River Rwizi Catchment area 30

Figure 4-1: Trend slope in precipitation 44

Figure 4-2: Standardized trend statistic (Z) in precipitation 45

Figure 4-3: Trend slope in PET 47

Figure 4-4: Standardized trend statistic (Z) in PET 49

Figure 4-5: Projected change in precipitation 52

Figure 4-6: Projected change in T_{max} 54

Figure 4-7: Projected change in T_{min} 56

Figure 4-8: Hydrographs of simulated flows using observed data- AWBM 58

Figure 4-9: Hydrographs of simulated flows using observed data- HMSV 59

Figure 4-10: Extracted high flow events- AWBM 61

Figure 4-11: Extracted high flow events- HMSV 64

Figure 4-12: Extracted Low flow events- AWBM 65

Figure 4-13: Extracted Low flow events- HMSV 67

LIST OF ACRONYMS

AWBM	Austrian Water Balance Model
CCAFS	Climate Change, Agriculture and Food Security
CMC	Catchment Management Committee
CMIP	Coupled Model Inter-comparison Project
CSD	Cumulative Sum of rank Difference
DRWM	Directorate of Water Resource Management
FAN – Stat	Frequency Analyses considering Non – Stationarity
GCM	Global Climate Model
HBV	Hydrologiska Byr˚ans Vattenavdelning
HMSV	Hydrological Model focusing on Sub-flows' Variation
IDW	Inversed Distance Weighting
IPCC	Intergovernmental Panel on Climate Change
JJAS	June, July, August and September season
JF	January and February season
MAM	March, April and May season
MWE	Ministry of Water and Environment, Uganda
NSE	Nash – Sutcliffe Efficiency
OND	October, November and December
PET	Potential Evapotranspiration
PGF	Princeton Global Forcing
POT	Peak-Over-Threshold
RCP	Representative Concentration Pathways

SRES	Special Report on Emissions Scenarios
SSPs	Shared Socio-economic Pathways
T_{max}	Maximum Temperature
T_{min}	Minimum Temperature
UNDP	United Nations Development Programme
UNCCP	Uganda National Climate Change Policy

ABSTRACT

There is lack of understanding on the impact of climate change on hydrological extremes of Rwizi Catchment. This threatens the sustainability of water to support socio- economic activities in the Rwizi Catchment. The procedure for conducting the study was guided by three objectives. Firstly, Trend analysis showed that precipitation mainly increased whereas Potential Evapotranspiration (PET) exhibited a decrease. The trend in both precipitation and PET were mainly insignificant. The second objective focused on establishing the climate change signals on precipitation and PET based on Global Circulation Models (GCMs) from Coupled Model Inter-comparison Project phase 5 (CMIP5) outputs. This was done by considering the Representative Concentration Pathways 4.5Wm^{-2} (RCP4.5) and 8.5Wm^{-2} (RCP8.5) scenarios. The precipitation and temperature of the 2050s and 2080s were projected to increase as to compared to the control period (1956–2002). Two conceptual hydrological models were calibrated and used for the impact assessment. Their difference in simulating the flows under future climate scenarios were also investigated. For the Austrian Water Balance Model (AWBM), the assembled mean projections of the high flow of 10- year return period for the 2050s and 2080s were projected to decrease. Whereas, for the Hydrological Model focusing on Sub-flows' Variation (HMSV), the assembled mean projections of high flows were projected to increase. The results for the low flows reveal decreasing low flow quantiles for AWBM for the 2050s and 2080s. However, for HMSV model, it showed increasing low flows quantiles. These impacts of climate change on the river flow show the need for a careful planning of relevant and appropriate adaption measures at a catchment scale.

Keywords: Climate change, Climate models, Hydrological models, Rwizi Catchment.

CHAPTER ONE: INTROCUCTION

1.1 Background of the Study

Water as a resource is an essential factor for the socio-economic development. Water resources planners (Mbaye, 2017) are facing considerable uncertainties related with the climate change impacts on water resources worldwide. These impacts are not only a threat to water sources but also to the country's development since they affect other key sectors such as agriculture, fisheries, forestry, energy, health, infrastructure and settlements (Taylor et al., 2014). Climate change is assumed to be as a result of increase in greenhouse gas concentrations in the atmosphere. The global rate of warming over the last 50 years has almost doubled that over the last 100 years (Trenberth et al., 2007). Due to global warming, the climate is projected to change and as such several of the hydrological cycle being one of the constituents of the components of the climate system will be severely perturbed (Nyeko- Ogiramoi, 2011).

The future of Uganda's water sources is being endangered due to pressure from anthropogenic activities (Nsubuga et al., 2014). This pressure is driven by several push factors, such as population growth, degradation of upland soils, and increasing rainfall variability due to climate change. These impact on key sectors of development (Ministry of Water and Environment (MWE), 2018) hampers efforts to reduce poverty, improve people's well-being and household incomes as Uganda's vision 2040.

The Rwizi Catchment Management Committee (CMC) and stakeholders are facing considerable uncertainties related with the future water resources (Nsubuga et al., 2014). Policies attempting to protect River Rwizi have often been weakly enforced

(Nsubuga et al., 2014). Furthermore, the MWE has embarked on water retention interventions in upland catchment areas to save river Rwizi that is threatened with extinction. This move which started with construction of water conservation structures that include earth and stone bunds, retention beaches, gabions and trenches in the upland catchment areas of this river in a bid to increase water storage in the soil so that water is available in wet and dry seasons has proven futile due to resistance from the community members, theft among others (MWE, 2018) performance report.

The potential hydrological impacts of climate change have proved to pose a significant challenge for water resource planning and management (Nyeko-Ogiramoi et al., 2010). These challenges are mainly extremes of climate such as severe droughts and prolonged wet spells, among others, which have very strong negative impacts on both natural and managed systems. It was reported by Nyeko-Ogiramoi (2011) that major water resources problems in the Rwizi catchment are related to both droughts and floods. These climatic changes are predicted to alter the catchment water balance in the future.

Several studies on climate change impacts have been carried out within the Rwizi Catchment (Nyeko-Ogiramoi et al., 2010; Onyutha et al., 2019; Ongoma et al., 2017). However, these studies had shortcomings, for instance, Nyeko-Ogiramoi et al. (2010) used the old generation of the Coupled Model Inter-comparison Project (CMIP3) data. There is a need to update the information on climate change using new generation (phase 5) of the Coupled Model Inter-comparison Project CMIP5) data outputs. However, Onyutha et al. (2019) used both CMIP3 and CMIP5 to investigated the uncertainties due to three downscaling techniques. The problem however, was that the

study was limited to changes in rainfall but not water resources in the catchment. The emphasis of Ongoma et al. (2017) was on changes in mean rainfall and temperature over E. Africa. However, only one station was considered in the entire Rwizi catchment.

Therefore, the aim of this study was to assess the impacts of climate change on the hydrological extremes of Rwizi Catchment by using the new generation of CMIP5. The findings from this study are relevant for planning adaptation measures with respect to the impacts of climate change on the water resources of the study area.

1.2 Statement of the Problem

Climate change is one of the most serious challenges facing the world today and is expected to impact hydrological processes such as precipitation, and evapotranspiration. This threatens the sustainability of the water to support socio-economic activities in the Rwizi catchment, with some of the focus areas in the Uganda's Vision 2040 being increased agricultural production, industrialization, and value addition to local products.

Past studies such as Nyeko-Ogiramoi et al. (2010) projected rainfall to increase by about 40% in Rwizi Catchment in the 2090s. Onyutha et al. (2019) projected 30% increase in the 2090s. However, these studies had shortcomings. Nyeko-Ogiramoi et al. (2010) used the old generation (Phase 3) of CMIP3. Onyutha et al. (2019) investigated the uncertainties due to three downscaling techniques and the study was limited to changes in rainfall.

Therefore, the study sets forth to assess the impact of climate change coupled with scenarios analysis on quantitative level of river flows in Rwizi catchment by use of CMIP5, GCMs outputs and hydrological modelling. This will give the Rwizi Catchment Management Committee (RCMC) and stakeholders an opportunity to predict and access future trends and possible management, planning and development approaches prior to execution.

1.3 Objectives of the Study

1.3.1 Main Objective

To assess the impacts of climate change on hydrological extremes of Rwizi catchment

1.3.2 Specific Objectives

i. To analyse trends in historical precipitation and Potential Evapotranspiration (PET)
ii. To establish projections of precipitation and Potential Evapotranspiration (PET) due to climate change impacts
iii. To investigate the changes in streamflow of river Rwizi under future conditions

1.4 Research Questions

The study was guided by the following set of questions;

i. Are there trends in historical (Precipitation and PET) data and are the trends significant?
ii. By how much will precipitation and PET change in the 2050s and 2080s?
iii. What is the extent of impact of climate change on water resources of River Rwizi?

1.5 Research Justification

The future projections of water resources in the Rwizi catchment are still unclear, and there is lack of understanding on the impact of climate change on water resources in

River Rwizi catchment. Currently the River Rwizi is classified as being in an alert state by the DWRM, based on the declining water levels during dry seasons hence the need for intervention that this study will make a contribution too.

1.6 Significance of the study

The climate change scenario analysis approach aims at enhancing the realization of integrated management of the Rwizi catchment since it provides an opportunity to water resource managers and users to forecast and evaluate the impacts of different possible future trends and management strategies before implementing them.

Assessing the extent of climate change on water resources using hydrological model will provide a basis for management, planning and development approaches.

1.7 Scope of the Study

i. Geographical scope

The study was limited to cover the upper River Rwizi Catchment.

ii. Time

The study was conducted from August, 2018 to August 2019.

iii. Models

- The study was limited to the application of lumped conceptual models.
- The study used a total of six GCMs of the CMIP5.

1.8 Conceptual framework

The study has conceptualized the impact of climate Change on the water resources in Rwizi catchment. This was based on the dependent and independent variables.

The framework (Figure 1.1) show how the linkages between climates change as an independent variable influences the river flow as the dependent variable.

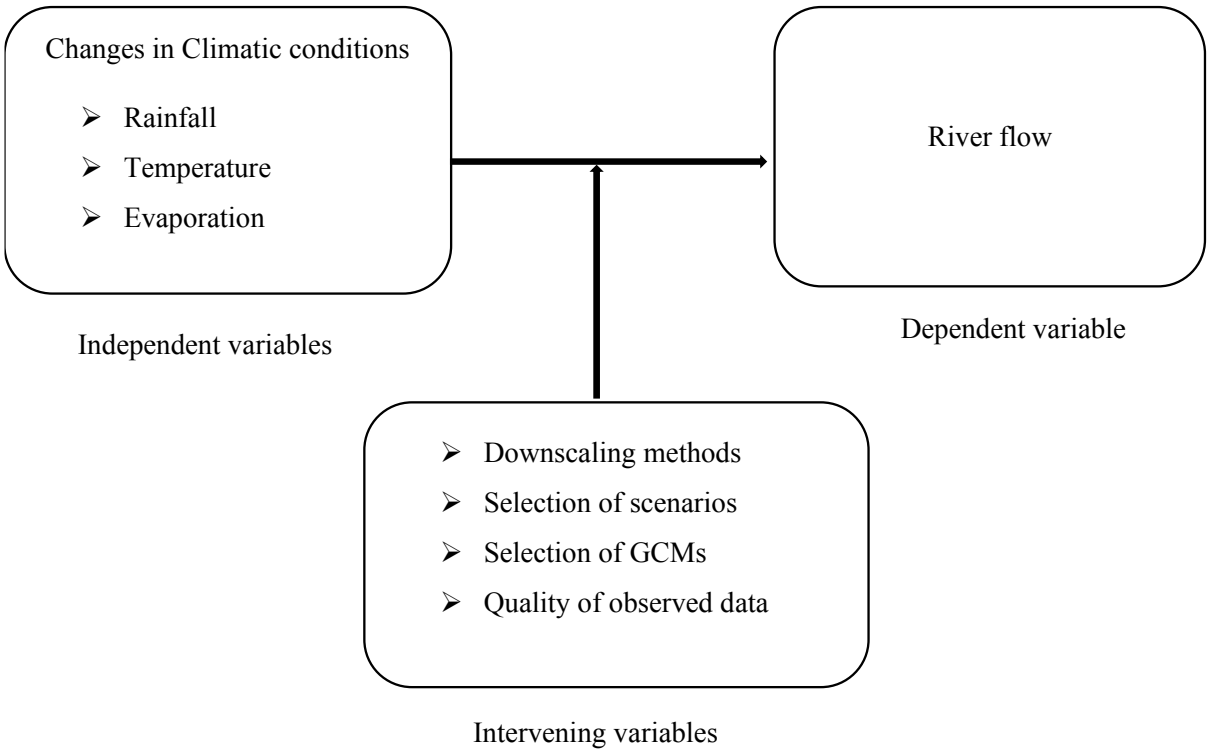

Figure 1-1: Conceptual framework of the study

CHAPTER TWO: LITERATURE REVIEW

2.1 Climate of Uganda

The climate of Uganda is naturally variable and susceptible to flood and drought events which have had negative socio-economic impacts in the past (Hepworth and Goulden, 2008). The most significant climate element is rainfall that plays a significant part in the economies of the majority tropical countries (Nsubuga et al., 2014). Uganda's rainfall displays a huge variance in time (temporal) and space (spatial) (Kangume, 2016).

2.1.1 Past studies on impacts of climate change on water resources in Uganda

Previous studies have examined the impacts of climate change on water resources in Uganda. Kangume, (2016) projected rainfall will increase by 0.34 mm per year under scenario A1B for River Malaba catchment which was averagely 1% less than the annual baseline period. However, Special Report on Emissions Scenarios (SRES) were adopted in this study and semi distributed model was used to assess the impacts of climate change.

Akurut et al. (2014) anticipated total annual precipitation to increase by less than 10% under scenario RCP4.5 and less than 20% for the RCP8.5 scenario over the 21st century. However, the study was limited to Lake Victoria, East Africa.

In the same region, Näschen et al., (2019) projected annual water yield and surface runoff to increase up to 61.6% and 67.8%, respectively, in Kilombero Catchment, Tanzania. However, the study used a semi-distributed Soil and Water Assessment Tool

(SWAT) to analyze the impacts on water resources under RCP4.5 and RCP8.5 scenarios.

Dessu and Melesse (2012), projected significant increase in flow volume of the Mara River flow at Mara Mines for the year 2046–2065 and 2081–2100.

2.2 Hydrology of River Rwizi Catchment

Rainfall distribution in the Rwizi catchment in temporal and spatial is the main effect on the catchment's hydrology (MWE, 2011) report. The catchment receives (Songa et al., 2015) mean annual rainfall that can go as low as 690mm. Nyeko-Ogiramoi (2010) deduced that annual rainfall can go as low as 800mm whereas Onyutha and Willems (2015), annual rainfall ranges between 995mm- 1097mm.

According to Onyutha et al., (2019), the historical daily rainfall intensity varies from 90 mm/month (Kamenyamigo station) to 120.6 mm/month (Rwoho station) with coefficient of variation (CV) 2.6 and 2.7, respectively over the period 1961–1990. Topography of the area also contributes to the rainfall distribution across the catchment such as hills in the west and flat areas of wetland and open water sources in the east of the catchment (Songa et al., 2015). The air temperatures vary with altitude. The average maximum (T_{max}) and minimum (T_{min}) temperatures is 28°C and 16°C, respectively (MWE, 2018). Dew-point temperature is 19°C and average temperature

is 24°C. January, February and March are the hottest months of the year (Songa et al., 2015).

2.3 Time series analysis

The rise in mean global sea levels is attributed to global warming which has resulted in greater climatic volatility such as changes in precipitation patterns and increased frequency and intensity of extreme weather events (Prasada and Addisu, 2013).

Trend analysis was essentially done to determine whether the change in climate data (rainfall and PET) throughout the past years was significant or not and to ensure that the selected period represents the historic climate data of the study area. There are many approaches that can be used to detect trends and other forms of non-stationarity in time series data.

2.3.1 Trend Magnitude

Trend magnitude indicates the amount by which the variable is anticipated to linearly change over a time unit of the observations (Onyutha, 2016a).

Trend magnitude is computed using Theil (1950) and Sen (1968). The slope is estimated by the equation below:

$$m = median\left(\frac{x_j - x_i}{j - i}\right) \forall i < j \qquad (2,1)$$

Where; x_j and x_i are the j^{th} and i^{th} observations respectively. m = Magnitude of linear trend. The slope is determined by the binomial distribution is robust estimate of the magnitude of the monotonic trend.

2.3.2 Trend direction

Trend direction is an expression of the dependence of the variable on time and this can be positive or negative (Onyutha, 2016a). This can be done by testing the H_0 (no trend) at the selected significance level α_s%. Several non-parametric methods exist for trend detection including the Mann–Kendall (MK) (Mann, 1945; Kendall, 1975), Spearman's Rho (SMR) (Spearman, 1904; Lehmann, 1975; Sneyers, 1990) and Cumulative Sum of rank Difference (CSD) test (Onyutha, 2016c; Onyutha, 2016d).

2.3.3 Past studies on time series analysis

Several studies have investigated historical trends in precipitation within Lake Victoria Basin and neighbouring areas. Nyeko- Ogiramoi et al. (2013) carried out a study on trend and variability in observed hydrometeorological extremes. It was obtained that there were positive trends, and no significance in the western parts of the Lake Victoria Basin where River Rwizi catchment is located. However, the emphasis of Nyeko-Ogiramoi et al. (2013) study was on investigation of the correlations between climate indices/solar activity and hydrometeorological extremes.

More to that, Kizza et al. (2009) investigated the temporal distribution of rainfall in Lake Victoria Basin on seasonal to annual time scales. The results showed positive trends, and no significance. However, only one station was considered within the upper Rwizi Catchment in Kizza et al. (2009) study despite its vast size. Such results may not be representative of the whole catchment under the study.

The study carried out by Onyutha (2018) analysed precipitation using short-term data observed over the entire Africa continent. The observed results indicated an increase

in annual and September–November precipitation of some areas along the Equatorial region (Lake Victoria basin) where the study area is located.

The mean surface temperature in the global has increased by 0.76°C over the past 150 years according to the Intergovernmental Panel on Climate Change (IPCC), (2007) and this is directly proportional to PET. However, due to wide regional differences, gaps in spatial coverage and temporal shortfalls in the data, global rainfall trends are complex (Halimatou et al., 2017). Data quality, data record length and selected time periods, etc (Majaliwa et al., 2015) are some of important factors to be considered in trend analysis.

2.4 Global Circulation Models (GCMs)

The primary source of information for constructing climate scenarios has been GCMs since they provide the basis for climate change impacts assessments at all scales, from local to global (Navarro-Racines et al., 2015). However, impact studies rarely use GCM outputs directly because errors in GCM simulations relative to historical observations are large (Ramirez-Villegas et al., 2013). For GCMs to present local subgrid-scale features and dynamics, there is a need to couple GCM with hydrological model which will provide a framework in which to conceptualize and investigate the relationship between climate and water resources (Dibike and Coulibaly, 2005).

2.4.1 Downscaling of GCMs

Downscaling relies on the assumption that local climate is a combination of large-scale climatic/atmospheric features (global, hemispheric, continental, regional) and local conditions (topography, water bodies, land surface properties) (Daniels et al., 2012).

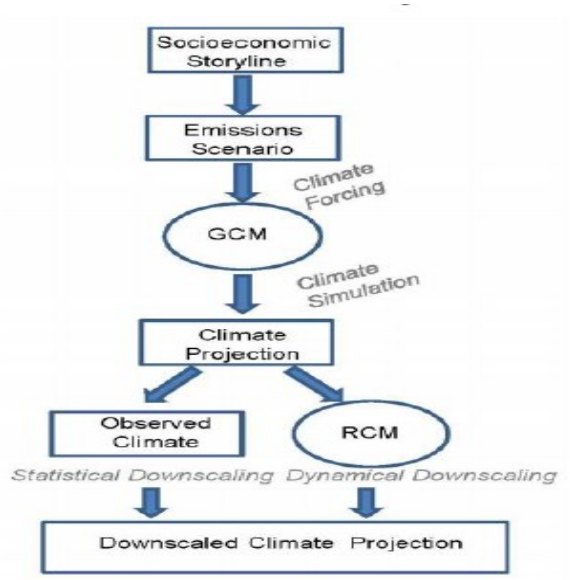

Figure 2-1: Illustration of developing downscaled climate projections

Source: (Trzaska and Schnarr, 2014)

The two principals of combining the information on local conditions with large-scale climate projections are as follows;

i. Dynamic Downscaling. This is the downscaling method of extracting local-scale information by developing and using limited-area models (LAMs) or regional climate models (RCMs) with coarse GCM data used as boundary conditions. The basic steps are then to use the GCMs to simulate the response of the global circulation to large-scale forcing and the nested RCM to account for sub-GCM grid scale forcing such as complex topographical features and land cover heterogeneity in a physically-based way and thus enhance the simulation of atmospheric circulations and climate variables at fine spatial scales (Coulibaly and Dibike, 2004). This method has numerous advantages but is computationally intensive and requires large volumes of data as well as

a high level of expertise to implement and interpret results, often beyond the capacities of institutions in developing countries.

ii. Statistical Downscaling. This is the most widely used downscaling technique. This is because they are computationally inexpensive in comparison to dynamical downscaling that require complex modeling of physical processes (Onyutha et al., 2016). Statistical downscaling involves the establishment of empirical relationships between historical large-scale atmospheric and local climate characteristics (U.S. Agency for International Development (USAID), 2014) report. Statistical downscaling encompasses a heterogeneous group of methods that vary in sophistication and applicability. These includes; linear methods, weather classifications and weather generators.

2.4.2 Performance of GCMs in Rwizi Catchment

Nonparametric statistical downscaling of daily rainfall time series from GCM runs was used by Nyeko-Ogiramoi et al. (2012) analyze the GCMs in reproducing rainfall over Lake Victoria Basin. Some of the GCMs used named according to IPCC model identity were; INM-CM3.0, MRI-CGCM2.3.2a, IPSL-CM4.1, CSIRO-Mk3.5a, CSIRO-MK3.0, BCCR-BCM2.0, CGCM3.1(T63), GFDL-CM2.1 and ECHAM5/MPI-OM. He found the best performing models were CSIRO-Mk3.5a, CSIRO-MK3.0 and ECHAM5/MPI-OM. The most inconsistent models over Rwizi catchment were INM-CM3.0, MRI-CGCM2.3.2a and IPSL-CM4.1. However, all the selected models were of old generation CMIP3 output.

Onyutha et al. (2019) investigated how well the climate models reproduce observed rainfall variability. He used CMIP3, CMIP5 and CORDEX model outputs. the CORDEX RCMs reproduce variability in daily rainfall over the study area, better than the CMIP3 and CMIP5 GCMs. This was because of higher spatial resolutions of the CORDEX RCMs than those of the CMIP3 and CMIP5 GCMs.

2.5 Selection of scenarios

In climate change impact assessment, climate scenarios are used to provide quantitative assessments of climate impacts. Climate scenarios are defined as possible representation of future climate which have been developed to be used exclusively in conjunction with investigating the potential impacts of anthropogenic climate change (IPCC, 2001). These scenarios take into account both human-induced climate change as well as natural climate variability. It is most common to develop climate change scenarios results from General Circulation Models (GCMs).

According to the Special Report on Emissions Scenarios (SRES) (IPCC, 2007), climate change scenarios are not forecasting of the future but instead they are potential future scenarios where every scenario represents a way the future might open out. Scenarios describe potential demographic conditions, environmental conditions, social conditions, policies, economic conditions and technologies. According to the IPCC (2007), the scenarios are described as follows:

i. A1 Scenario: “Describes a potential world of extremely fast growth in the economy, worldwide population that reaches the peak in mid-century and

reduces after that, and the fast introduction of latest and additional competent technologies.

ii. A2 Scenario: “Describes a very diverse continent. The fundamental theme is independence and protection of local identities.

iii. B1 Scenario: “Describes a unified globe whose population growth is as low as in the A1 scenario but with fast change in structures in the economy in the direction of economical service and information, among decrease in intensity of material and the clean and resource-efficient introduction of technologies.

iv. B2 Scenario: “Describes a globe whose importance is on economic, social and environmental sustainability local solutions.

The IPCC for its fifth Assessment Report (AR5) in 2014 adopted the Representative Concentration Pathways (RCPs) which are four greenhouse gas concentration trajectories. They describe four possible climate futures, all of which are considered possible depending on how much greenhouse gases are emitted in the years to come.

Climate scenarios are based on economic and population growth. The four RCPs, RCP2.6, RCP4.5, RCP6, and RCP8.5, are named after a possible range of radiative forcing values in the year 2100 relative to pre-industrial values +2.6, +4.5, +6.0, and +8.5 W/m^2, respectively. the scenarios are described as follows;

i. RCP8.5 predicts a future of high range emission scenario (possible development for high population numbers, high fossil/coal use)

ii. RCP6.0 predicts medium range emission scenario (low-medium baseline scenario or high mitigation scenario)

iii. RCP4.5 predicts a future of medium range emission scenario (high mitigation scenario)

iv. RCP2.6 predicts a future of low range mitigation scenario.

Climate change scenarios demonstrate possible futures of global warming which can be addressed by planned actions such as encouraging green energies. Preventive scenarios can be compared to other scenarios like RCP4.5 and RCP2.6 in order to have an overview on their effects when it comes to reducing the global warming (Socolow and Pacala, 2006). The concentration of carbon dioxide has reached about 375 ppm. Limitation of emission of carbon dioxide has a lot of issues such as cost which can make it hard to reach an agreement between governments and agencies. So, the 550-ppm policy is one of the feasible policies that can be considered by policy makers and scientists to project future climatic conditions.

Shared Socio-economic Pathways (SSPs) are scenarios of projected socio-economic global changes up to 2100 (Fricko et al., 2016). SSPs were developed as a joint community effort over the last years to provide a toolkit for the climate change research community to carry out integrated, multi-disciplinary analysis (Fricko et al., 2016). The SSPs are based on five narratives describing alternative socio-economic developments which includes; Sustainable development (SSP1), Middle-of-the-road development (SSP2), Regional rivalry (SSP3), Inequality (SSP4) and Fossil-fuelled development (SSP5) (Riahi et al., 2017).

2.7 Hydrological modelling for climate change impact investigation

The reasons for modelling climate change impact investigations of water systems is to understand how the catchment responds to a variety of hydrologic conditions (Alamou et al., 2017). There are two main categories of Hydrologic model; Physically based and Lumped conceptual models.

Physically based models are useful for answering science and management questions related to hydrological processes, the impact of climate and land-use changes, as well as managing and supporting water resources (Sazib, 2016). These models are data intensive and often require specific transformation of available data sets to convert to the form required by a model for example; HEC-HMS (Bedient and Huber, 1992), SWMM (Huber and Roesner, 2012), TOPMODEL (Beven and Kirby, 1979; Beven et al., 1986), e.t.c.

Lumped conceptual models are the ones whose parameters do not vary spatially within the catchment and response is evaluated only at the outlet, without explicitly accounting for the response of individual sub catchments (Boughton, 2009). For example, AWBM (Boughton, 2004), TANK model (Sugawara and Funiyuki, 1956), Sacramento Soil Moisture Accounting Model (SAC-SMA) (Brazil and Hudlow, 1981), SIMHYD model (Porter, 1972; and Porter and McMahon, 1975), SMAR model (O'Connell et al., 1970) e.t.c.

Advantages of conceptual models over physically based models

i. Their parameters do not represent physical features of hydrologic processes hence easy to calibrate

ii. They require less parameters hence applicable in data scarcity areas

iii. Discharge prediction is at outlet only

Due to difficulties in calibration and model input requirements, conceptual models were adopted in this study.

2.7.1 Lumped conceptual modelling for climate change impact investigation

Several studies have shown that have applied lumped conceptual model in assessing the impact of climate change on water resources.

Alamou et al. (2017) applied four conceptual models which were ModHyPMA, Hydrologiska Byr˚ans Vattenavdelning (HBV), Austrian Water Balance Model (AWBM) and Simplified form as HYDROLOG (SimHyd) to evaluate future water availability in the Mékrou catchment, Benin under climate change scenarios. Based on the results obtained, the conceptual models showed good performance in simulation of future streamflows.

Nyeko-Ogiramoi (2011) also assessed future streamflows using conceptual model (VHM model) under scenarios A2, A1B and B1 for the 2050s and 2090s in River Katonga and Rwizi catchment. The model performed well in evaluating hydrological impact examination.

2.7.2 Lumped conceptual models

The types of some of lumped conceptual models are;

i. Austrian Water Balance Model (AWBM)

The AWBM (Boughton, 2004) is a catchment water balance model that relates daily rainfall and evapotranspiration to runoff, and calculates losses from rainfall for flood hydrograph modelling.

The model uses 3 surface stores to simulate partial areas of runoff. The water balance of each surface store is calculated independently of the others (Figure 2.2). The model calculates the moisture balance of each partial area at either daily or hourly time steps. At each time step, rainfall is added to each of the 3 surface moisture stores and evapotranspiration is subtracted from each store. The water balance equation is:

$$Store_n = Store_n + rain - evap \qquad (2,2)$$

Where $n = (1\ to\ 3)$

If the value of moisture in the store becomes negative, it is reset to zero, as the evapotranspiration demand is superior to the available moisture. If the value of moisture in the store exceeds the capacity of the store, the moisture in excess of the capacity becomes runoff and the store is reset to the capacity.

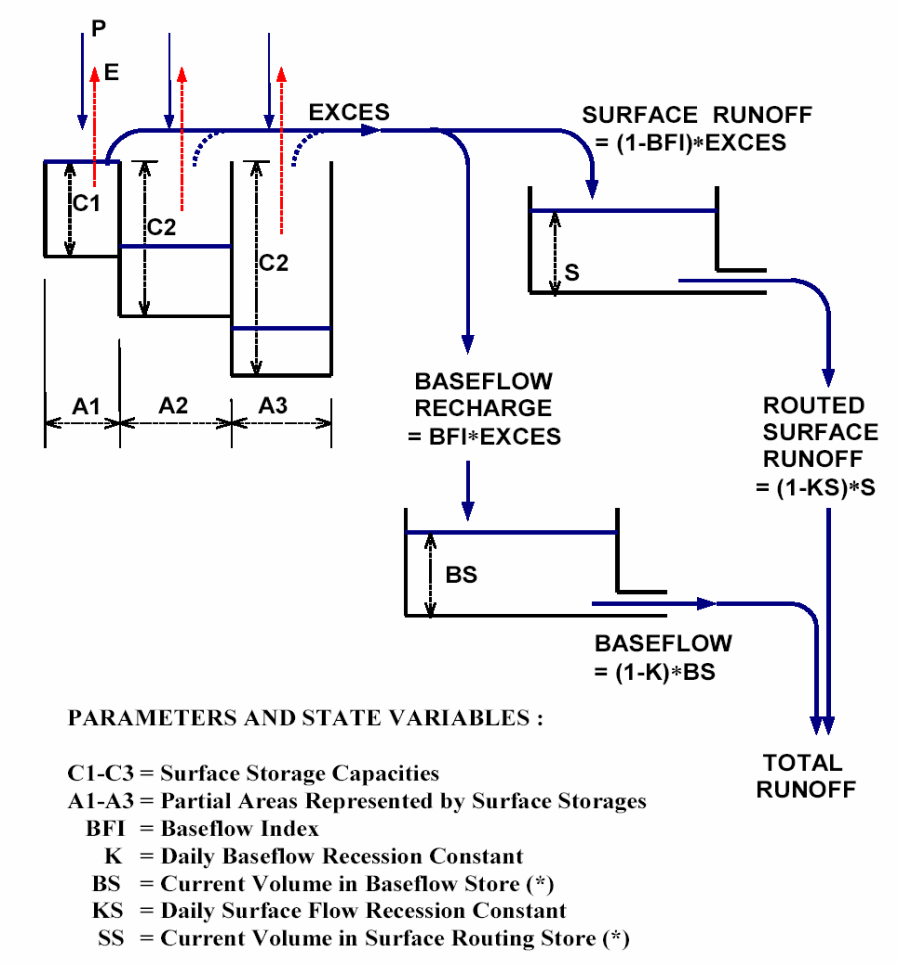

Figure 2-2: AWBM model structure (Source: Boughton, 2004)

The number of surface stores chosen is a pragmatic choice to reflect sufficient skill to simulate runoff without adding too may parameters and facing the risk of over-optimization. Rainfall is added to each of the surface stores and evapotranspiration is subtracted at each time step. The rainfall in exceeding the storage capacity flows to the groundwater store, and the remainder becomes surface runoff.

ii. TANK

The TANK model (Sugawara and Funiyuki, 1956) is a simple structure model developed in Japan and it has been applied to many river basins investigations. It is

efficient and powerful tool in rainfall-runoff simulation and verification. It assumed the watershed as a series of storage vessels and the data required for model calibration are only precipitation, runoff and evaporation.

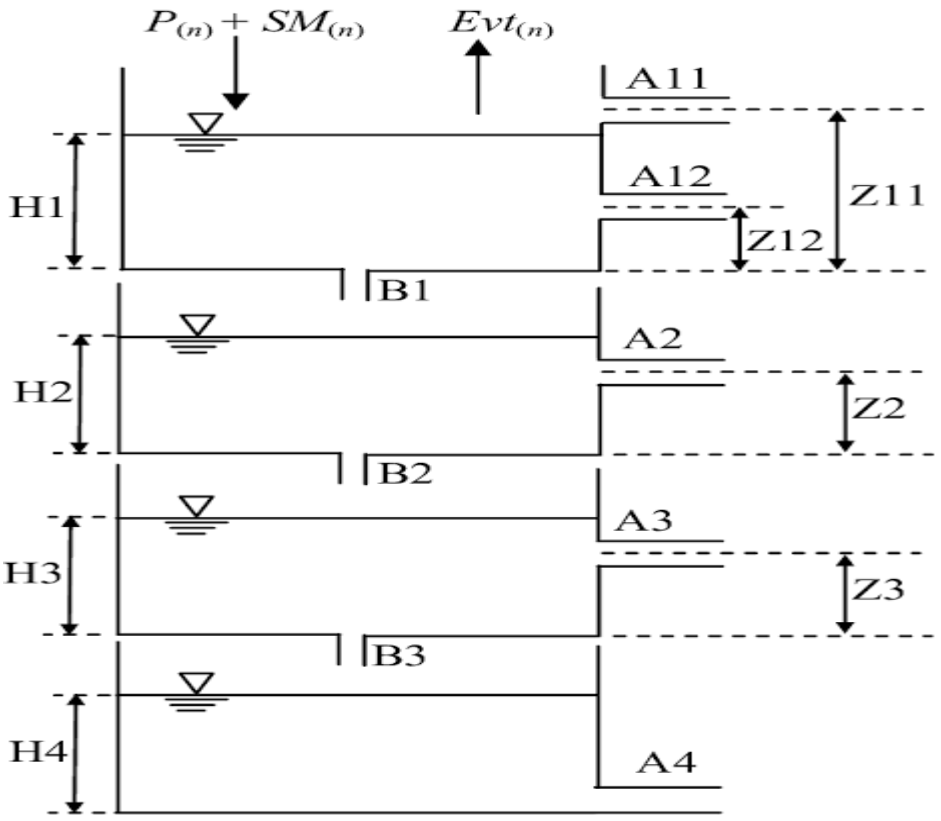

Figure 2-3: TANK model structure (Source: Podger, 2004)

- The total runoff is calculated as the sum of the runoffs from each of the tanks. The runoff from each tank is calculated as;

$$q = \sum_{x=1}^{4} \sum_{y=1}^{nx} (C_x - H_{xy}) a_{xy} \quad (2,3)$$

Where q is the runoff depth in mm, C_x the water level of tank x, H_{xy} the outlet height and a_{xy}, is runoff coefficient for the respective outlet of tank.

- The evapotranspiration is calculated using Beken's (1979) equation;

$$ETA = ETP \times (1 - \exp(-\alpha \sum_{x=1}^{4} C_x) \quad (2,4)$$

Where *ETA* is the evapotranspiration in mm, α the evapotranspiration coefficient (0.1) and C_x the water level of tank.

- The infiltration in each tank is calculated using:

$$I_x = C_x B_x \tag{2,5}$$

Where I_x is the infiltration in mm, C_x the water level of tank x and B_x the infiltration coefficient tank x.

iii. Soil Moisture Accounting and Routing (SMAR)

The SMAR (O'Connell et al., 1970) is a conceptual rainfall-runoff model. The water balance component of the model is based on the "Layers Water Balance Model" (Nash and Sutcliff 1969). In the SMAR model, it is assumed that the basin structure is analogous to a vertical stack of horizontal soil layers, each of which can contain a certain amount of moisture. The SMAR model has nine parameters and these parameters may be fixed at appropriately chosen values, while the values of the rest are usually estimated empirically by optimization to minimize the objective function in the form of the sum of the squares of the errors between the observed and estimated flows. The surface run-off generated from the landscape is routed (attenuation and lag) to the catchment outlet using the linear cascade model of Nash (1960). The model was obtained as a general solution relating a given input of unit volume to a given output as in equation 1.

$$h(t) = \frac{1}{t}\int_{t-1}^{t} \frac{1}{K\Gamma(n)} \exp\left(\frac{-\tau}{K}\right)\left(\frac{\tau}{K}\right)^{n-1} d\tau \tag{2,6}$$

where, t = simulation time step (d), τ = time (S), $K_1 = K_2 = \ldots\ldots = K_n = K$ are the storage coefficients of n linear reservoirs in cascade, $h(t)$ = ordinates of the pulse

response function (d^{-1}) and $\Gamma(n) = \int_0^\infty \exp(-\tau)\tau^{n-1}d\tau$ is the complete Gamma function (dimensionless).

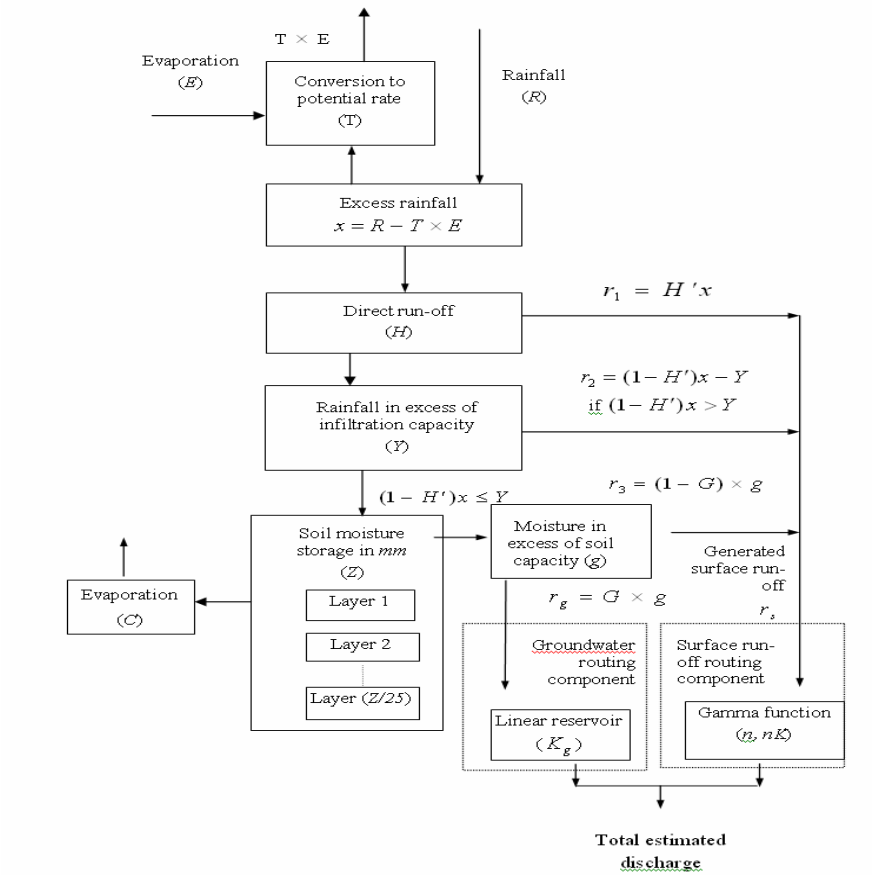

Figure 2-4: Structure of the SMAR model (Source: O'Connell et al., 1970)

iv. Simplified form as HYDROLOG (SIMHYD)

The SIMHYD (Porter, 1972; and Porter and McMahon, 1975) is a simplified version of the daily time series rainfall-runoff model HYDROLOG, and the more recent MODHYDROLOG (Chiew and McMahon, 1991). The SIMHYD model has seven parameters as compared to the seventeen (17) parameters required for HYDROLOG and the nineteen (19) for MODHYDROLOG.

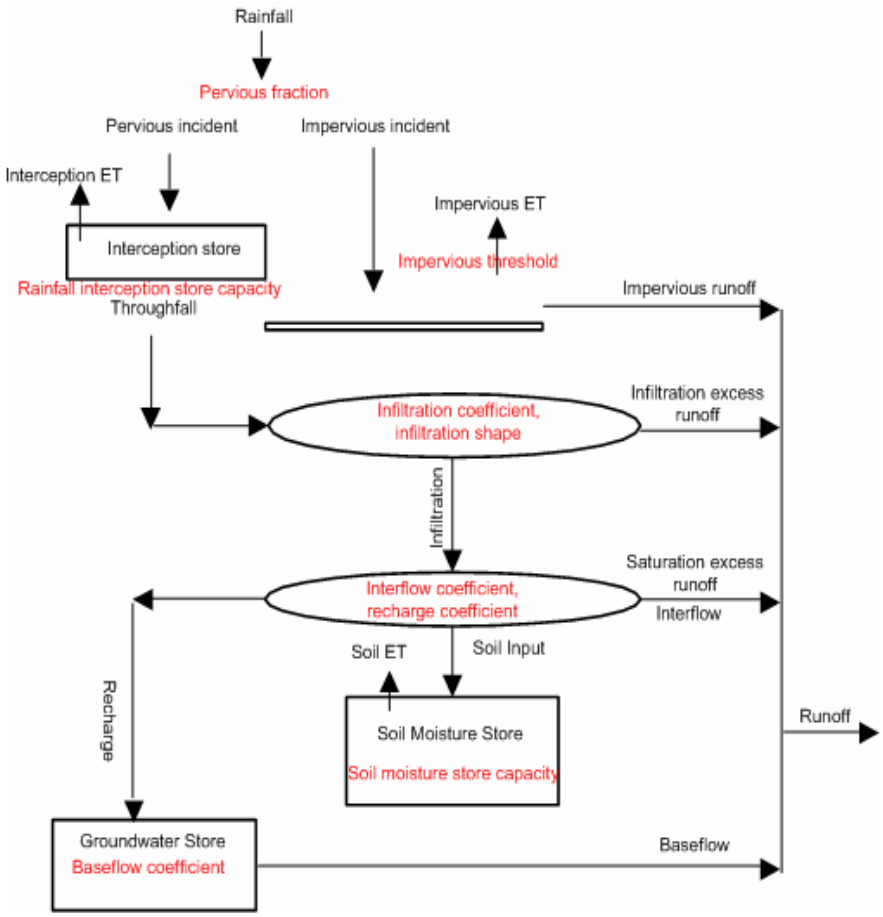

Figure 2-5: Structure of the SIMHYD model (Source: Porter, 1972)

v. Hydrological model focusing on sub-flows' variation (HMSV)

The HMSV model focuses on the separation of flows into sub flows (Onyutha, 2019). The Model splits the run off flows into base flow (Q_{bf}), inter flow (Q_{if}) and over land flow (Q_{of}). The HMSV model performs well in reproducing quantiles of both high flows and low flows (Onyutha, 2019). The input parameters are Potential Evapotranspiration (PET), River flow (Q) and precipitation (P).

The output of the HMSV is the total simulate streamflow (Q_{sim}) from the three different sub flows.

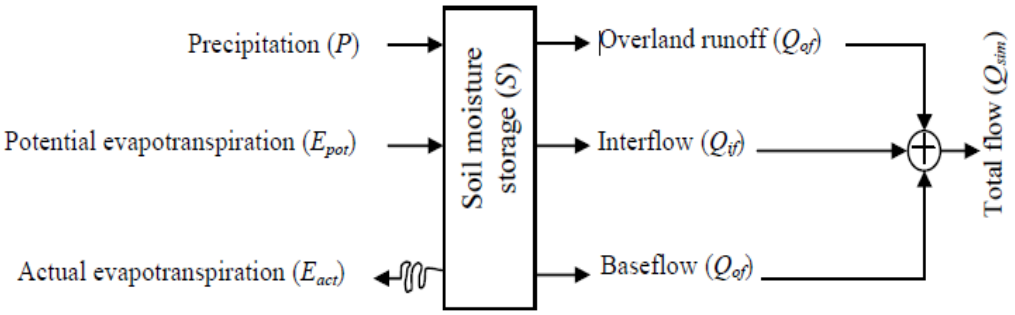

Figure 2-6: Schematic representation of HMSV (Source: Onyutha, 2019)

The model adds or subtracts moisture from the soil water storage based on the magnitude of P(t) and $E_{pot}(t)$ such that;

$$S(t) = S(t-1) + P(t) - E_{pot}(t) \qquad if\ P(t) \geq E_{pot}(t) \qquad (2,7)$$

$$S(t) = S(t-1) \times e^{-\frac{PET(t)-P(t)}{Smax}} \qquad if\ P(t) < E_{pot}(t) \qquad (2,8)$$

Where S_{max} denotes the maximum limit of soil moisture storage deficit (mm/day).

The selected model has to be;

i. Reasonably cheap
ii. the need for compatibility of the model structure with data requirements
iii. ability of the model to simulate extreme events

2.7.3 Calibration of the conceptual models

Model calibration is a process of optimizing or systematically adjusting model parameter values to get a set of parameters which provides the best estimate of the observed runoff. Practically, all rainfall runoff models must be calibrated to produce

reliable estimates of runoff since there is slight evidence identified of strong links between physical characteristics and the parameters of rainfall runoff models (Beven, 1989).

When calibrating a model, it should always be noted that there is tradeoff which will be driven by the purpose of the model.

2.7.4 Validation of the conceptual models

Model validation is a process of using the calibrated model parameters to simulate runoff over an independent period outside the calibrated period to determine the suitability of the calibrated model for predicting runoff over any period outside the calibration period. If there is limited data, the validation can be performed by testing shorter periods within the full record (Beven, 1989). Model validation is one of the most important steps in rainfall- runoff modelling as the performance of the calibrated model in the validation periods gives confidence in the modelling results when the calibrated model is used for simulating streamflow outside the measured streamflow period or when projecting streamflow under climate change scenarios.

2.8 Climate change impact investigation on streamflow

For quantile estimation, the extreme events are required to be independent and identically distributed. To extract the extreme events from the full time series, Peak Over Threshold (POT) approach (Smith, 1985; Lang et al., 1999) or the Annual Maxima Method (AMM) (Langbein, 1949) can be used. For the AMM, the maximum event in each hydrological year is extracted. The AMM yields events with strong independence. However, the number of the extreme events tends be limited especially

for data of short record length (Onyutha, 2017). To generate an adequate number of events to provide a reasonable definition of extreme value region, the POT method is often preferred to the AMM approach. Extraction of independent extreme events can be done using the method of POT based on the independence criteria. The independence criteria, based on daily time scale, is as follows:

(i) the time in between the two events should not be less than the stipulated value;

(ii) the extracted event should not be less than the specified threshold; and

(iii) the independency ratio should not be greater than a stipulated value.

CHAPTER THREE: MATERIALS AND METHODS

3.1 Introduction

This chapter outlines and shows the materials and methods used in this study. This includes the means by which the researcher was able to assess the study area and compile data for analysis. This study is based on secondary data.

3.1.1 Study area

River Rwizi flows eastwards from the hilly south-western area of Uganda, eventually draining into Lake Victoria. There are several lakes in the lower reaches of the catchment, namely Lake Mburo, Lake Nakivale, Lake Kachera and Lake Kijanebalola. The altitude varies from 1,380 to 2,171 metres above sea level.

The river crosses through districts of Buhweju, Sheema, Bushenyi, Ntungamo, Isingiro and Ibanda before discharging into Lake Mburo. The upper Rwizi catchment considered in this study covers an area of 2098Km^2. The delineated map showing the study area is shown in figure 3.1.

Figure 3-1: River Rwizi Catchment area

3.2 Data

The data used in this study were observed and GCMs data. The datasets were rainfall, river flow and PET data.

3.2.1 Rainfall data

The daily rainfall data were obtained from Ministry of Water & Environment (MWE), Metrological department. There was a total of ten (10) rainfall stations considered in this study. Five stations were located within the catchment. The rest were around the catchment as shown in Table 3.1. However, some rainfall gauges had missing data records which were improved by interpolation technique. Thus, the method of Inversed Distance Weighting (IDW) (Eqn. 3.4), originally used by Shepard (1968), was adopted to estimate missing data values for the data with some missing records.

$$P_{\times} = \frac{\sum_{i=1}^{n} {}^{P_i}/_{d_i}}{\sum_{i=1}^{n} {}^{1}/_{d_i}} \tag{3.1}$$

Where;

P_x is the unknown rainfall value,

P_i is the known rainfall value at station *i,*

n is the total number of stations with known variable value,

d_i is the weight assigned to variable value at station *i* (e.g. distance between station with unknown and known rainfall)

Table 3.1: Stations within and around Rwizi catchment

S/No.	Latitude	Longitude	Station ID	Description
1	-0.617	30.65	90300030	Mbarara Met
2	-0.717	30.35	90300190	Ndeizha- Mbarara
3	-0.6	30.53	90300250	Mbarara Stock Farm
4	-0.567	30.32	90300210	Rubare Farm
5	-0.417	30.58	90300470	Rubindi
6	-0.467	30.67	90300220	Rubaya Gombolola HQ
7	-0.733	30.53	90300270	Bugamba Forest Station
8	-0.833	30.15	90300340	Kitunga (Muntuyera) High School
9	-0.817	30.55	90300420	Kikunda Rwoho
10	-0.88	30.27	90300450	Ntungamo

3.2.2 Observed flow data

The observed flow data were obtained from MWE, department of Water Resource Management. Mbarara Water Works (81224) gauging station (0.616, 30.643) along Mbarara- Kabale road was considered as our discharge station for the Rwizi upper catchment. The flow daily series data considered were from 1956 to 2002.

3.2.3 Potential Evapotranspiration (PET)

The daily time step series for PET were computed using Hargreaves formula (Hargreaves and Allen, 2003).

$$ET_o = 0.0023\ R_a(T_{mean} + 17.8)(T_{max} - T_{min})^{0.5} \times 0.408 \quad (3.2)$$

Where;

ET_o: Potential Evapotranspiration (mm)

T_{mean}: Mean temperature (^oC)

T_{max} and T_{min}: Maximum and Minimum temperature (^oC)

R_a: is the extraterrestrial radiation ($MJm^{-2}\ day^{-1}$), a function of location given by (Hargreaves and Allen, 2003).

$$R_a = 15.392 d_r(\omega_s sin\emptyset sin\delta + cos\emptyset cos\delta sin\omega_s) \quad (3.3)$$

where ϕ is the latitude of the location and d_r is the relative distance between the earth and the sun given by:

$$d_r = 1 + 0.033\cos\left(\frac{2\pi J}{365}\right) \quad (3.4)$$

where J is the Julian day to estimate incoming solar energy

δ is the solar declination (radians) defined by:

$$\delta_r = 0.4093\sin\left(\frac{2\pi J}{365} - 1.405\right) \quad (3.5)$$

and ω_s is the sunset hour angle (radians) given by;

$$\omega_s = cos^{-}(-tan\emptyset tan\delta) \quad (3.6)$$

However, since the observed temperature data for the study area were not available, freely available daily data (T_{min} and T_{max}) of the Princeton Global Forcing (PGF) were downloaded from internet link http://hydrology.princeton.edu/data/pgf/0.5deg

[accessed on 25/5/2019]. Although the PGF data runs from 1948 to 2002, the T_{min} and T_{max} over the period 1956-2002 were used to compute daily PET.

3.2.4 Downscaled climate data

The downscaled data (temperature and precipitation) were downloaded online via the link http://ccafs-climate.org/ [accessed on 30/5/2019]. These datasets were of monthly time scale for the period 2050s and 2080s.

3.3 Time series analysis

In this study, both trend magnitude and direction were considered to analyse historical trends in precipitation and PET.

3.3.1 Trend magnitude

The trend slope was computed using Equation. 2,1 (Sen 1968; Theil 1950). This method has been applied in other similar works (Omondi et al., 2013; Kizza et al., 2009; Onyutha, 2017; Aguilar et al., 2005, 2009)

To evaluate the significance of m from (Eq. 2.1), the hypothesis H_0 (no trend) and the alternative hypothesis H_1 (trend) can be tested at the selected significance (α). In this study, seasonal and annual of both precipitation and PET at each station, m (Eq. 2-1) was computed and its significance assessed by testing the H_0 $(m = 0)$ at $\alpha = 0.05$. The α=0.05 was considered because it is commonly used (Kizza et al., 2009; Nsubuga et al 2011; Nyeko-Ogiramoi et al., 2010).

3.3.2 Trend direction

The non-parametric Cumulative Sum of rank Difference (CSD) test recently developed by Onyutha (2016a) was adopted in this study because it makes use of both graphical diagnoses and statistical analyses. The CSD trend analysis approach was implemented in a tool referred to as CSD-NAIM. This tool was downloaded online via the link: https://sites.google.com/site/conyutha/tools-to-download (accessed: 18 July, 2019). The CSD approach (Equation 3.8) (Onyutha, 2016a). Given a series, x of sample size n, y can be taken as the replica of x such that for $1 \leq i \leq n$, the ith transformed data point d_i can be obtained using (Onyutha 2016a)

$$d_i = 2\sum_{j=1}^{n} sgn_1(y_j - x_i) - (n - \sum_{j=i}^{n} sgn_2(y_j - x_i)) \tag{3.7}$$

Where,

$$sgn_1(y_j - x_i) = \begin{cases} 1 & if\ (y_j - x_i) > 0 \\ 0 & if\ (y_j - x_i) \leq 0 \end{cases}$$

$$sgn_2(y_j - x_i) = \begin{cases} 1 & if\ (y_j - x_i) = 0 \\ 0 & if\ (y_j - x_i) < 0\ or\ (y_j - x_i) > 0 \end{cases}$$

From (Eq. 3.7), the rank difference d_i can be used to detect trends. Trend can be tested both graphically and statistically using di (Eq. 3.7). Graphically, the diagnosis of the change in the series shall be determined from the cumulative sum S_i of the rank difference d_i (Eq. 3.7) can be obtained using;

$$S_i = \sum_{j=1}^{i} d_j \qquad for\ 1 \leq i \leq n \tag{3.8}$$

Statistically, the CSD trend statistic T shall be computed using

$$T = \frac{6}{(n^3-n)} \sum_{i=1}^{n=1} S_i \quad (3.9)$$

Where S_i is from (Eq. 3.8)

$T > 0$ indicate positive trends whereas $T < 0$ indicate negative trends.

3.3.3 Standardization of trend test statistics Z

This follows the standard normal distribution mean (variance) of zero (one) and is computed using Eqn. (3.10). considering $Z_{\alpha/2}$ as the standard normal variance at the selected x, the H_0 (no trend) is rejected if $|Z| \geq Z_{\alpha/2}$. Otherwise, the H_0 is not rejected (Onyutha 2016a).

$$Z = \frac{T}{\sqrt{V}} \quad (3.10)$$

Where;

$$V = \frac{1}{n-1}\left(1 - \frac{10}{17}e^2 - \frac{7}{17}e\right) \times |1 + \frac{2}{n(n^2-3)} \times \sum_{k-1}^{n-2}(n-k)^3 r_k^{\alpha}| \quad (3.11)$$

Whereas, e as the measure of ties is given by;

$$e = \frac{-1}{n^2-n}(n - \sum_{i-1}^{n}\sum_{j-1}^{n} sgn_2(y_j - x_i)) \quad (3.12)$$

And r_k^{α} as the $lag-k$ correlation coefficient (r_k) significant at α.

The linear trend slope (m), Eqn. (2.1) is computed before r_k

For, $1 \leq i \leq n$, the detrended series C is computed from;

$$C_i = x_i - m \times i \quad (3.13)$$

Given $C^{\#}$ is the mean of $C_i's$, the values of the r_k can be calculated using Eqn. (3.14) (Salas et al. 1980)

$$r_k = \frac{\frac{1}{(n-k)}\sum_{i-n}^{n-k}(C_i - C^{\#})(C_{i+k} - C^{\#})}{\frac{1}{n}\sum_{i-1}^{n}(C_i - C^{\#})^2} \quad (3.14)$$

And the $100(1-\alpha)\%$ confidence interval limits (Cl_{lim}) for testing the significance of r_k can be computed using Eqn. (3.15) (Anderson 1941);

$$Cl_{lim} = \frac{-1 \pm Z_{x/2}\sqrt{n-k-1}}{n-k} \quad (3.15)$$

In Eqns. (3.14)- (3.15), k should be set to vary from $k = 1$ up to n-2 (Onyutha 2016a).

3.4 Projection of future climate conditions from GCMs outputs

3.4.1 Climate scenarios selection

The SRES and SSPs scenarios were not used in this study because they are not present in Climate Change, Agriculture Foot Security (CCAFS) portal. Hence, the RCPs were adopted in this study. RCP8.5 and RCP4.5 scenarios were considered because they explain the most "likely to happen" development paths (medium and high development path) in Uganda (Kangume, 2016).

3.4.2 Selection of GCMs used in this study.

The CMIP5 GCMs were selected based on recommendations from past studies. Akurut et al. (2014) projected the potential impacts of climate change on precipitation using new generation of GCMs over Lake Victoria which is within the same region of this

study. The bcc-csm1-1 model used in this study was among the other models recommended by Akurut et al. (2014). More to that, Onyutha et al. (2019) used and recommended bcc-csm1-1, miroc-esm-chem, csiro-mk3.6.0, ipsl-cm5a-lr, gfdl-esm2g and mpi-esm-lr. Ongoma et al. (2017) used and recommended csiro-mk3.6.0 as the best performing model. The CMIP5 modes were adopted as shown in Table (3.2).

Table 3.2: Basic information of the GCMs used in this study

Model Name	**Institution**	**Resolution (Lon x Lat)**
bcc-csm1-1	Beijing Climate Center, China Meteorological Administration, China.	2.81^{o} x 2.79^{o}
csiro-mk3-6-0	Commonwealth Scientific and Industrial Research Organization/Queensland Climate Change Centre of Excellence.	1.88^{o} x 1.88^{o}
gfdl-esm2g	NOAA Geophysical Fluid Dynamics Laboratory, USA	2.50^{o} x 2.00^{o}
ipsl-cm5a-lr	Institute Pierre-Simon Laplace, France	3.75^{o} x 1.89^{o}
miroc-esm-chem	Atmosphere and Ocean Research Institute (The University of Tokyo), National Institute for Environmental Studies, and Japan Agency for Marine-Earth Science and Technology, Japan.	2.81^{0} x 2.79^{o}
mpi-esm-lr	Max Planck Institute for Meteorology, Germany	1.88^{o} x 1.87^{o}

3.4.3 Data for future climatic conditions

As stated in section 3.2.4, the climate data were obtained in already downscaled form. However, they were of monthly time scale and the downscaled data were at a regional scale. There was a need to adopt the monthly climate change projection signals to the daily time scale as required by the hydrological model. In other words, the reginal scale was to be reduced to catchment level. To do so, the daily observed data were converted to monthly data. Next the ratio of monthly scenarios to the observed monthly data was considered as the perturbation factor. Each value of the observed data within each month was multiplied by the corresponding perturbation factor to obtained scenarios in future climatic data of the periods 2050s and 2080s. For temperature, absolute perturbation was considered to obtain series of the future climatic condition.

3.5 Selection of lumped conceptual models used for this study

The choice of model starts with the model being able to solve the problem in question (Laio et al. 2009). The task was to choose the model which can give the best solution objective without compromising the accuracy of the results.

From the above basis, Onyutha (2016b) found AWBM to perform well under both moderate and extreme flow conditions in Blue Nile Basin. Whereas HMSV performed well in reproducing quantiles of both high flows and low flows. Therefore, HMSV and AWBM were adopted in this study since they are capable to simulate extreme flow events which are important for a careful analysis as required in this study. The model was obtained from Rainfall Runoff Library (RRL) of the "eWater Toolkit" from the link https://toolkit.ewater.org.au/. [accessed on 30/6/2019]

3.5.1 Setting up and Evaluation

The daily time series of PET, rainfall and runoff were converted in the format (tts files) required by the conceptual rainfall-runoff model (AWBM & HMSV) and used as the model input. The initial conditions and parameters were set.

The models were calibrated between 01/01/1956 to 31/12/1989 and validated was done for the period 01/01/1990 to 31/12/2002. Nash- Sutcliffe Efficiency (NSE) (Nash and Sutcliffe, 1970) was used to evaluated model performance in this study. NSE is defined as;

$$NSE = 1 - \left[\frac{\sum_{i=1}^{n}(Q_{o,i}-Q_{s,i})^2}{\sum_{i=1}^{n}(Q_{o,i}-\overline{Q_{o,i}})^2}\right] \quad (3.16)$$

Where;

RE: Nash-Sutcliffe coefficient of efficiency [-]

$Q_{o,i}$: observed streamflow at the ith time interval (m^3/s)

$Q_{o,i}$: simulated streamflow at the ith time interval (m^3/s)

$\overline{Q_{o,i}}$: mean of the observed streamflow (m^3/s)

n : the number of time steps of the observations [-]

3.6 Future river flows

The daily time series of downscaled data (PET and precipitation) were used as inputs in the hydrological models to obtain future flows through simulation. The future PET time series as stated before were computed from projected T_{max} and T_{min}. Simulation

of the future streamflows was done under scenarios RCP4.5 and RCP8.5 for the 2050s and 2080s.

3.6.1 Analysis of the extent of climate change on river flow

To carefully analyze the extent of climate change impact on river flow, the Peak Over Threshold (POT) events were extracted from observed simulated flow as well as the simulated flow of the future climatic conditions. FAN-Stat tool (Onyutha, 2017) was used. FAN-Stat stands for Frequency Analysis considering Non-Stationarity. The independency criteria for the extraction of POTs using the FAN-Stat Version 2 followed a study by Onyutha (2019). The comparison between observed and future flows was made within the context of frequency analysis. The POT's of observed and future flows were compared on a return period basis to estimate the impact of climate change on the river flow.

Considering hydrological drought conditions, the given discharge or river flow time series Q was transformed by (1/Q). The extreme value analysis of low flow was done in the similar way as that for high flow. This was because the use of (1/Q) makes the low flows to follow the generalized Pareto distribution or exponential instead of Weibull or Fréchet distribution as clearly shown by Onyutha (2016a).

CHAPTER FOUR: DISCUSSION AND PRESENTATION OF RESULT

4.1 Introduction

This section summarizes the results of this study and provides explanatory analysis to highlight key findings. These results were generated following the methods highlighted in Chapter Three.

4.2 Time series analysis

4.2.1 Trends in precipitation

Figure 4.1 shows slope trends in precipitation of the study area. Figure 4.1a shows a negative trend. This indicates decreasing trend (precipitation) in the season of January and February (JF). The highest precipitation decreases (at a rate of about -1.636mm/year) was obtained in the southern part of the study area in Ntungamo.

Figure 4.1b shows positive trend which indicates increase in precipitation in the season of March, April and May (MAM). The largest increase in precipitation (at a rate of about 4.413mm/season) was obtained in the south eastern part of the study area in the district of Mbarara around Bugamba forest and Kikunda Rwoho station. This could be due to the role of Bugamba and Rwoho forests in attracting rainfall over the study area.

Figure 4.1c shows positive trends which indicate increase in precipitation in June, July, August and September season (JJAS). However, the trends recorded in JJAS season were much lower than those of MAM season. This could be due to the fact that JJAS is a dry season. The lowest positive (increase) trend was obtained over the north

eastern part of the catchment in Mbarara district around Rubindi and Rubaya Subcounties.

Figure 4.1d shows positive and negative trends. This designates increasing and decreasing trend (precipitation) in October, November and December (OND) season. The decreasing trends were obtained in the western part of the study area over the district of Buhweju and Bushenyi. However, the increasing trends were obtained in the district of Mbarara around Rwoho and Bugamba forests.

Figure 4.1e shows positive and negative trends of annual precipitation. The negative (decreasing) trend (at a rate of about -1.555mm/year) was obtained in the western part of the study area over the districts of Buhweju, and Bushenyi. This could be due to the fact that the areas are on a leeward (drier) side of Mt. Rwenzori which has an influence on precipitation. However, the positive (increasing) trend (at a rate of 3.845mm/year) was obtained in the southern part of the study area in Mbarara District around Bugamba and Kikunda forests which may have a positive influence on rainfall.

This study was consistent with the results from a recent study by Onyutha (2018) who obtained about 5mm/year increase in precipitation from 1901 to 2015 over the Equatorial region around Lake Victoria in East Africa where the study area is located. However, the seasons for which most parts of the study area exhibited a decrease in precipitation was JF, followed by JJAS and finally OND.

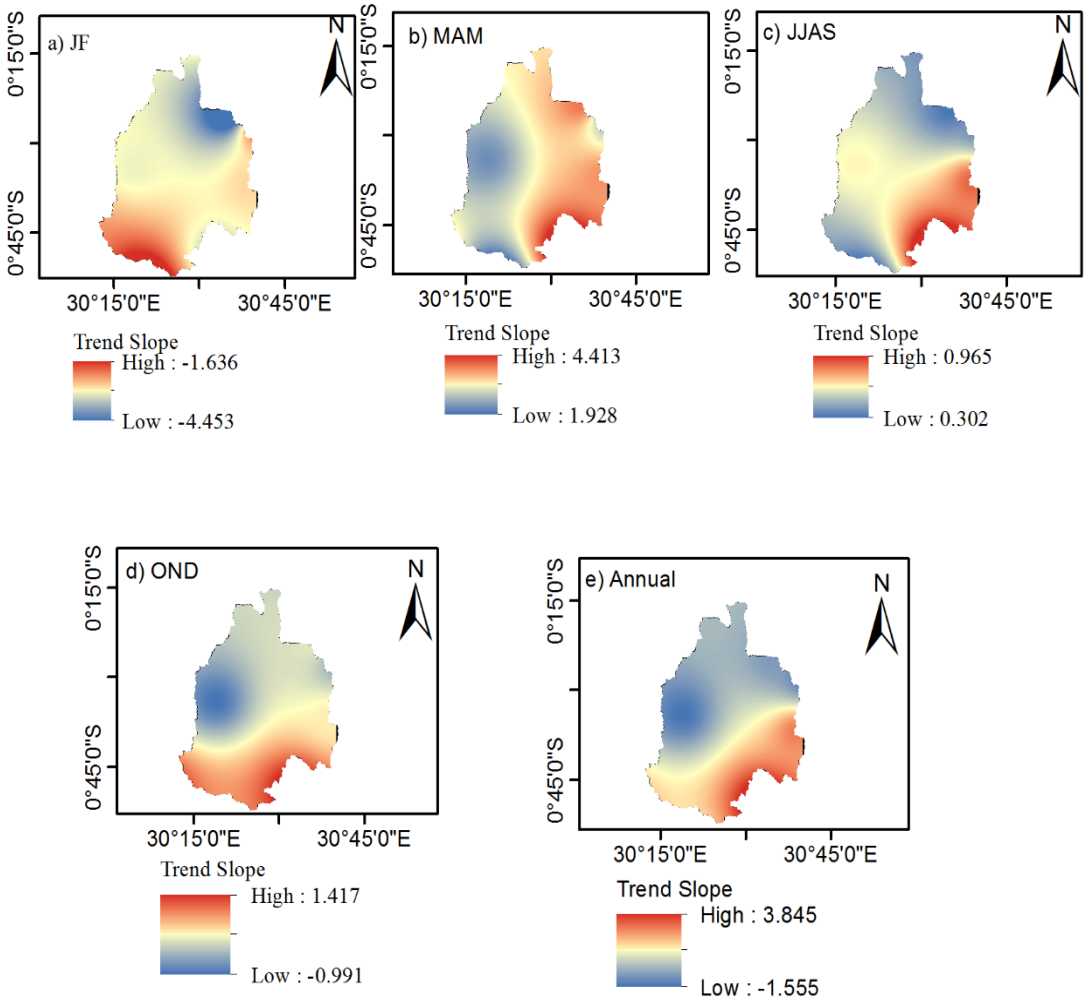

Figure 4-1: Trend slope in precipitation

Figure 4.2 shows the insignificance in annual and seasonal precipitation trends for the period 1979-2002. The null hypothesis H_0 (no trend) was rejected ($P < 0.5$) for;

i. Precipitation decrease in the season of JF in the entire study area, as well as annul in the western and north eastern parts of the study area (Figure 4.2a).

ii. Precipitation increase in MAM, JJAS and OND season in the south eastern and southern parts of the study area (Figure 4.2b, c, d)

iii. An increase in annual precipitation in the south eastern part of the study area around Bugamba and Rwoho forests.

Past studies on trend analysis have also indicated no significant trends in the study area. Kizza et al. (2009); Onyutha (2016a); Nyeko- Ogiramoi et al. (2013) did not find evidence of significant trends in the study area.

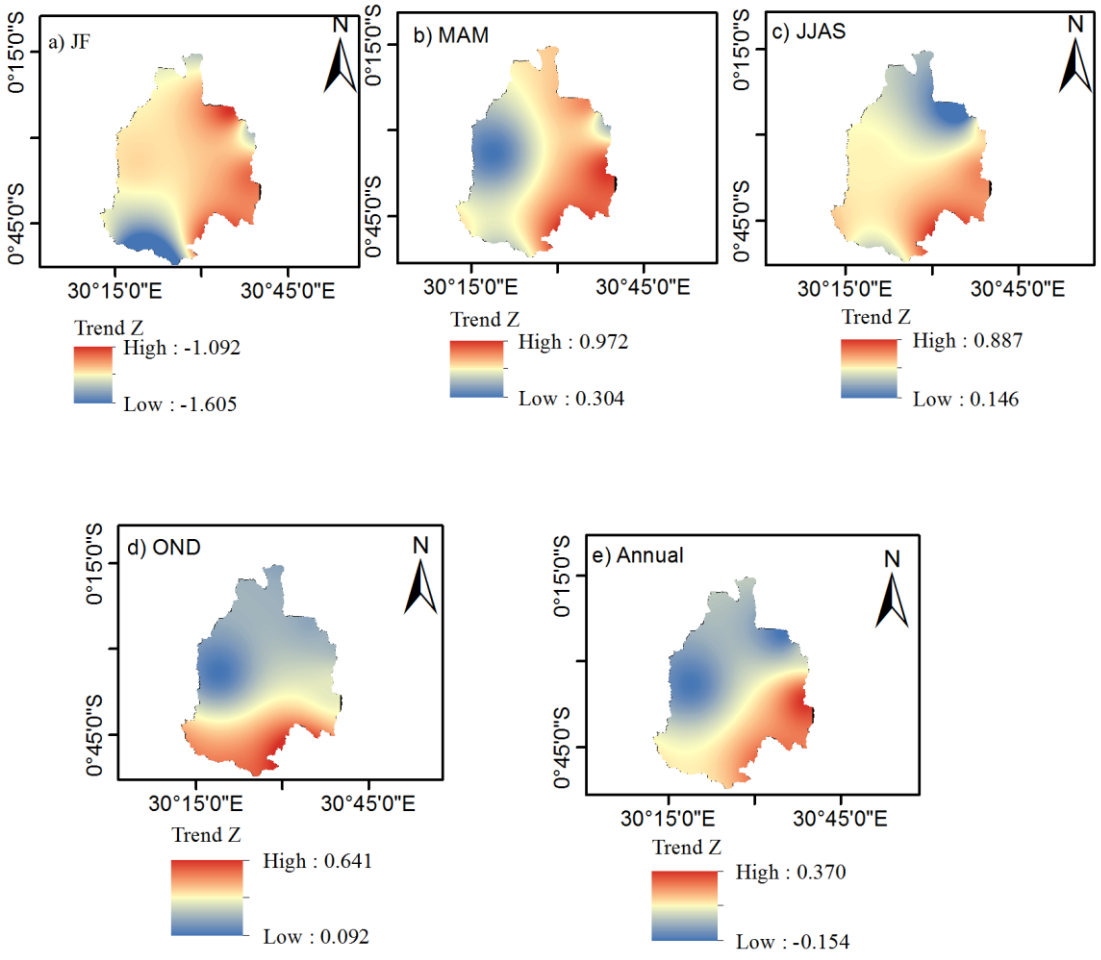

Figure 4-2: Standardized trend statistic (Z) in precipitation

4.2.2 Trends in Potential Evapotranspiration (PET)

Figure 4.3 shows the trend slopes in PET. Figure 4.3a shows the negative (decrease) trend for JF season. The lowest decrease in PET (at a rate of about -2.944mm/year) was obtained in south western part of the study area in Ntungamo district. This may be due to the negative (decreasing) precipitation as obtained over same part of the study area (Figure 4.1a).

Figure 4.3b shows the positive (increase) trend in PET for the MAM season. The lowest increase was obtained in the western part of the study area over the district of Buhweju and Bushenyi. This could be due to the fact that the areas are on a leeward side of Mt. Rwenzori which receives less (decreasing) precipitation (Figure 4.1b).

Figure 4.3c shows Positive and negative trend was obtained in JJAS. The negative (decrease) trend were obtained in the north eastern part of the study area in Rubindi and Rubaya subcounties. This related to the lowest obtained precipitation as indicated in Figure 4.1c.

Figure 4.3d shows positive and negative trend for OND season. The negative (decrease) trend was obtained in western and eastern side of the study area. This related to Figure 4.1d that indicate decrease trend in precipitation over the same location of the study area.

Figure 4.3e shows negative (decrease) trend for annual PET over the entire catchment. The lowest decrease was obtained in north eastern and south western side of the study area. The negative trends in annual PET was associated with maximum degradation of vegetation cover especially Papyrus and poor land use practices in the study area

(Atwongyeire et al ., 2018; Ojok et al., 2017) which have a negative impact on evapotranspiration.

More to that, the decreasing trend was also attributed to increasing Temperature globally (Nsubuga et al., 2011; Kizza et al., 2009; Nyeko-Ogiramoi et al., 2010). Decreasing trend in PET indicates a decrease in net total radiation and a significant decrease in wind speed which results into less/ no precipitation.

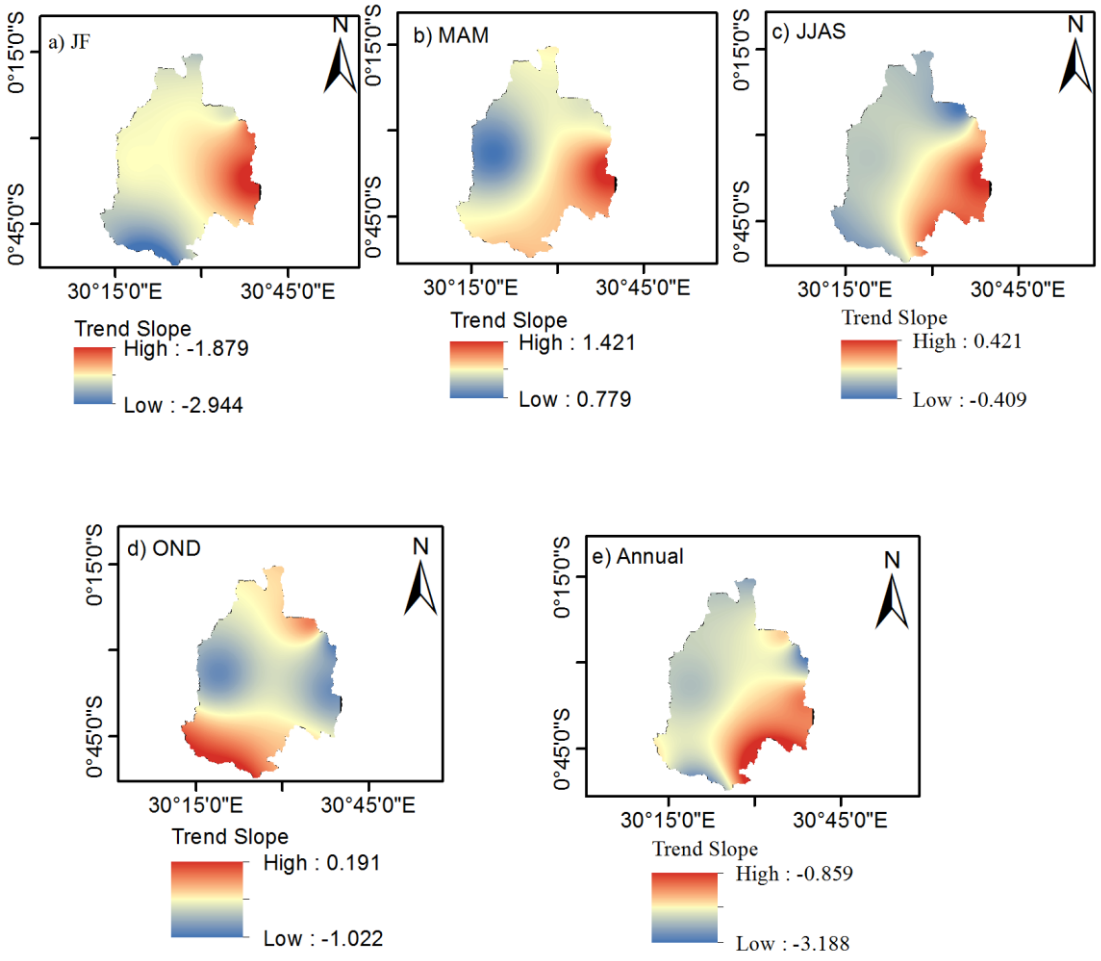

Figure 4-3: Trend slope in PET

Figure 4.4 shows the insignificance in PET trends. The threshold levels for Z at a significance level α = 5% is +1.96 and −1.96. The lower negative value (-2.148) in JF season (Figure 4.4a) fell outside the confidence interval limits. Hence, indicating significant trend in the north east part of the study area in Rubindi subcounty. The H_0 (no trend) was rejected (P<0.5) for;

iv. PET decrease in annual (Figure 4.4e) in the entire study area, as well as JF season in the western, central and eastern parts of the study area (Figure 4.4a).

v. Precipitation increase in MAM season in the southern part of the study area (Figure 4.4b)

vi. An increase in JJAS precipitation in the southern part of the study area around Ntungamo district.

PET values indicate the amount of water that has been lost through evapotranspiration and has to be replaced by precipitation, the findings of this study are consistent with the past studies that have indicated no significant trends in precipitation over the study area (Kizza et al., 2009; Onyutha, 2016a; Nyeko- Ogiramoi, 2011).

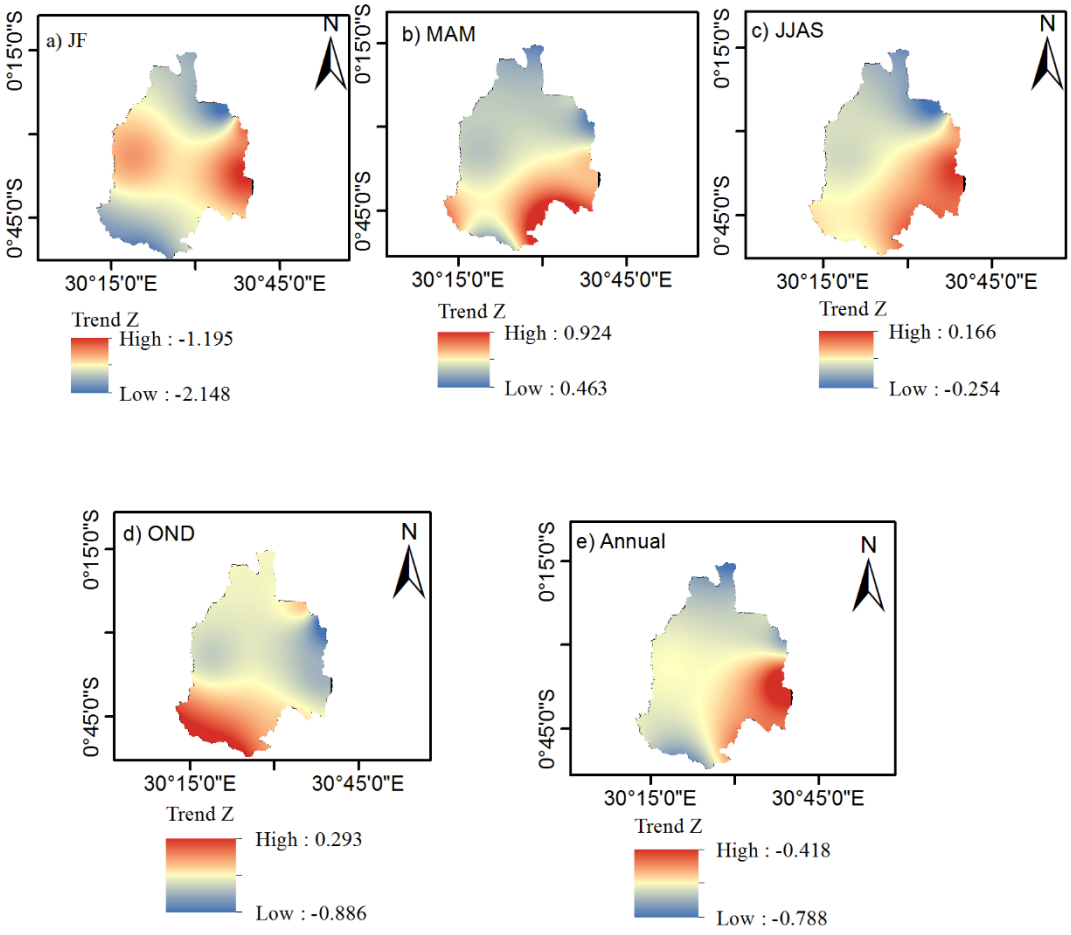

Figure 4-4: Standardized trend statistic (Z) in PET

Precipitation and PET are the most important components of the hydrological cycle. The results at a particular location gives an insight on whether the place is becoming wetter or drier than the past conditions which requires real consideration in terms of water management under rainfed agriculture which is mostly practiced in Rwizi Catchment.

4.3 Projected change in future climatic conditions

4.3.1 Projected change in precipitation

Figure 4.5 shows projected change in precipitation under scenario RCP4.5 in the 2050s and 2080s under the RCP4.5 and RCP8.5. Figure 4.5a, b shows projected precipitation in the 2050s and 2080s period under the RCP4.5. The average projected increase in precipitation in the 2050s and 2080s was about 24% and 30%, respectively. However, it was obtained that the mean precipitation will decrease by about 7.5% (4.953mm) and 3.6% (2.397mm) in the 2050s and 2080s, respectively in the JJAS season. This indicates that long dry spells are projected in future under RCP4.5 scenario.

Figure 4.5c, d shows projected precipitation under the RCP8.5 in the 2050s and 2080s. The average projected increase in precipitation in the 2050s and 2080s was by about 30% and 48%, respectively. For the dry JJAS season in RCP8.5 scenario, the total seasonal precipitation amount is expected to decrease by about 6.6% (4.321mm) in the 2050s, and increase by about 3.9% (2.582mm) in the 2080s. This indicates that the dry season in the 2050s will be drier than that of the current conditions under RCP8.5 scenario.

Based on the precipitation results, it was obtained that on average, that the tendency of a linear relationship between the observed and simulated future precipitation increase with increase in the grid size of the model. This implies that model resolution is vital in determining the GCM performance in projecting future precipitation.

Other studies have also projected increase in future precipitation in the River Rwizi catchment. Using old generation GCMs of CMIP5, Nyeko-Ogiramoi et al. (2012) and Nyeko-Ogiramoi (2011) projected an increase in precipitation in Rwizi catchment over the period 2050s and 2080s. Nyeko-Ogiramoi et al. (2012) projected mean precipitation to change by -10% to 57% for the 2050s and -10% to 82% for the 2080s over Ruizi catchment. However, Onyutha et al. (2019) projected precipitation to increase by 11.7- 43.6% and 14.2 to 40.6% over the period of 2050s and 2080s, respectively under RCP8.5 scenario which is in close agreement with this study. However, the emphasis of Onyutha et al. (2019) was on investing the uncertainties due to downscaling techniques and only Rwoho Forest station was considered which could not represent the changes in the whole catchment. The findings of this agree with Mcsweeney et al. (2008) that reported that various parts of Uganda will experience increase in precipitation. The differences in future changes in precipitation frequency for the 2050s and 2080s, for RCP4.5 and RCP8.5, is not large.

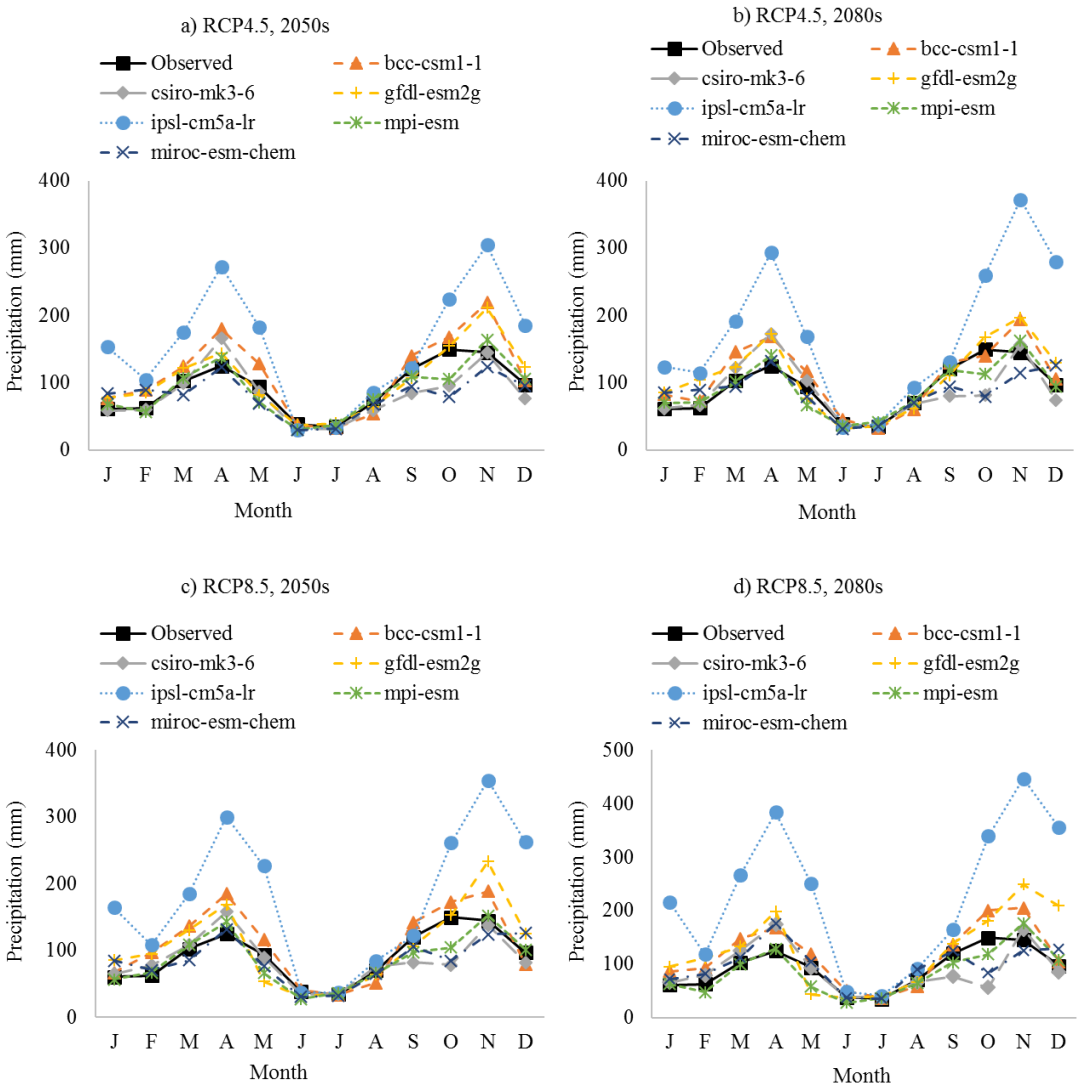

Figure 4-5: Projected change in precipitation

4.3.2 Projected change in temperature

Figure 4.6 shows projected T_{max} in the 2050s and 2080s periods. Figure 4.6a, b shows projected T_{max} in the 2050s and 2080s under the RCP4.5. By averaging the changes for all the months, the projected increase in T_{max} in the 2050s and 2080s was by about

0.7% and 2%, respectively. However, it was obtained that the mean T_{max} will decrease by about -1.0% (-0.281^{0}C) and 0.2% (0.055^{0}C) in the 2050s and 2080s, respectively in the OND season. Figure 4.6c, d shows projected T_{max} in 2050s and 2080s under the RCP8.5. The average projected increase in T_{max} in the 2050s and 2080s was by about 4.0% and 10.0%, respectively. However, the lowest increase for T_{max} was obtained in OND season where the average projected increase will be by about 2.1% (0.585^{0}C) and 7.5% (2.043^{0}C) in the 2050s and 2080s, respectively.

As T_{max} increases, the rate of evapotranspiration (PET) increases. Evaporation increases because there is a higher amount of energy available to convert the liquid water to water vapor. This vapour condenses to precipitation. All models were under and over the observed data for precipitation except in the 2080s under the RCP8.5 were all models were over the observed data.

Overestimation of future T_{max} totals for the csiro-mk3-6 model can be attributed to the small grid sizes that allow simulating different T_{max} patterns over the entire study area. Therefore, the relationship between the observed and simulated future T_{max} increase with decease in the grid size of the model. This implies that model resolution is vital in determining the GCM performance in projecting future T_{max}.

This study was consistent with Nyeko-Ogiramoi (2011) who projected T_{max} to increase by 0-2.5% and 0-5% in 2050s and 2080s, respectively. However, he used old generation of CMIP3 GCMs in his study.

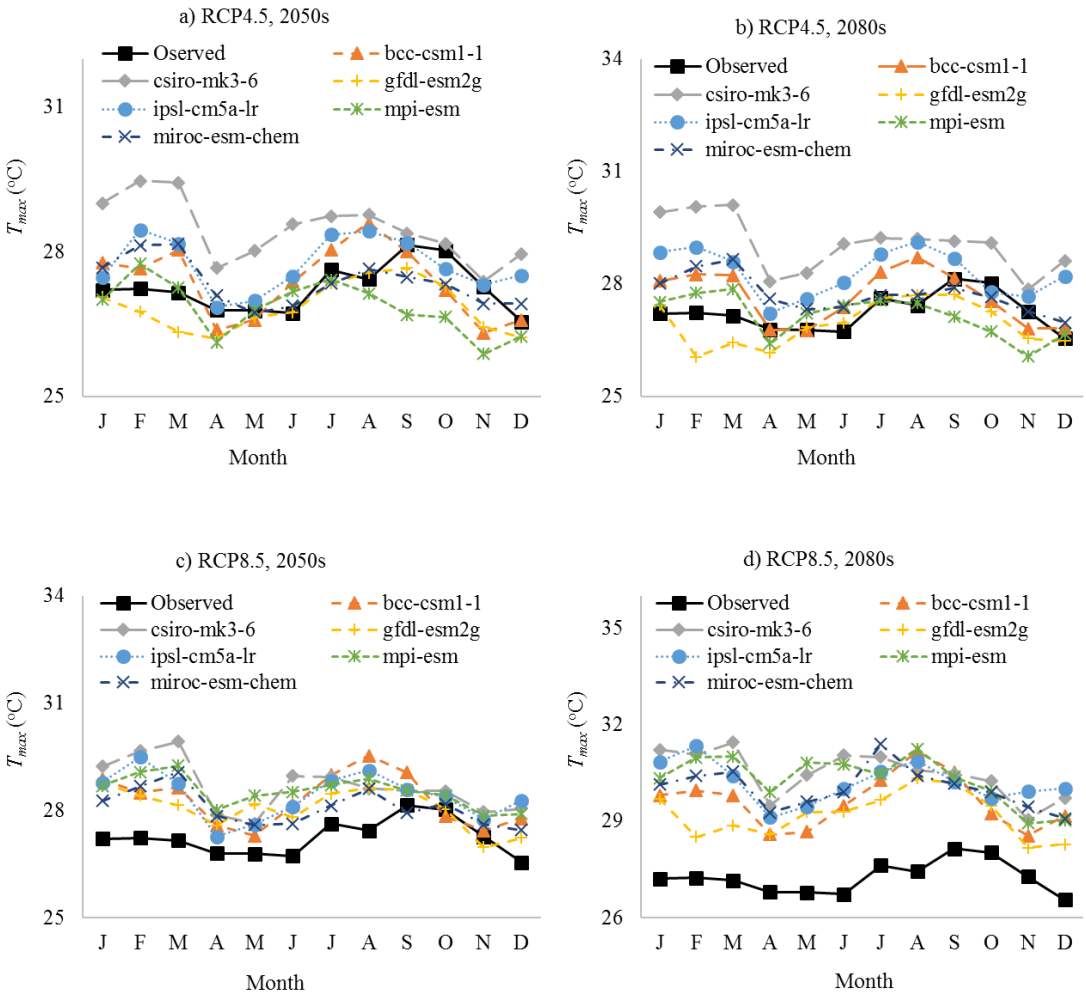

Figure 4-6: Projected change in T_{max}

Figure 4.7 shows projected T_{min} in the 2050s and 2080s periods. Figure 4.7a, b shows projected T_{min} under the RCP4.5. The average projected increase in T_{min} in the 2050s and 2080s was by about 8.7% and 12.2%, respectively. However, the lowest increase in T_{min} was obtained in JJAS season where the average projected increase will be by about 6.3% (0.889^{0}C) and 8.8% (1.257^{0}C) in the 2050s and 2080s, respectively.

Figure 4.7c, d shows projected T_{min} under the RCP8.5. The average projected increase in T_{min} in the 2050s and 2080s was by about 14.6% and 28.3%, respectively. However, the lowest increase in T_{min} was obtained in JJAS season by about 11.4% (1.621^{0}C) in

the 2050s. For the 2080s, the projected lowest increase T_{min} was by about 23.2% (3.348^0C) in OND under the RCP8.5 scenario.

There was a slight difference between the findings of this study with that of Nyeko-Ogiramoi (2011) who projected T_{min} to change by -3.5°C to about 9°C in the 2050s under the A2 and A1B scenarios, respectively, whereas -1.5°C to 9°C change was projected in 2090s under A2 and AIB scenarios within the study area. This was due to the fact that he used old generation of CMIP3 GCMs and SRES scenarios. In the same region, Egeru et al. (2019) projected T_{min} to increase by 1.8 °C and 2.2°C in 2050s and 2080s, respectively under RCP4.5, whereas under RCP8.5 scenarios, T_{min} was projected to increase by 2.1 °C and 4.0°C in 2050s and 2080s, respectively in sub humid region of Uganda. This is due to the fact that climatic conditions of the study areas are different from this one. Other studies projected mean annual temperature to increase in Uganda. McSweeney et al. (2008) projected temperature to increase by about 1.0 to 3.1°C in the 2050s. Whereas McSweeney et al. (2010) projected about 1.4 to 4.9 °C increase in the 2080s in Uganda. Unlike the precipitation anomalies, monthly temperature shows a fairly consistent trend irrespective of climate scenario.

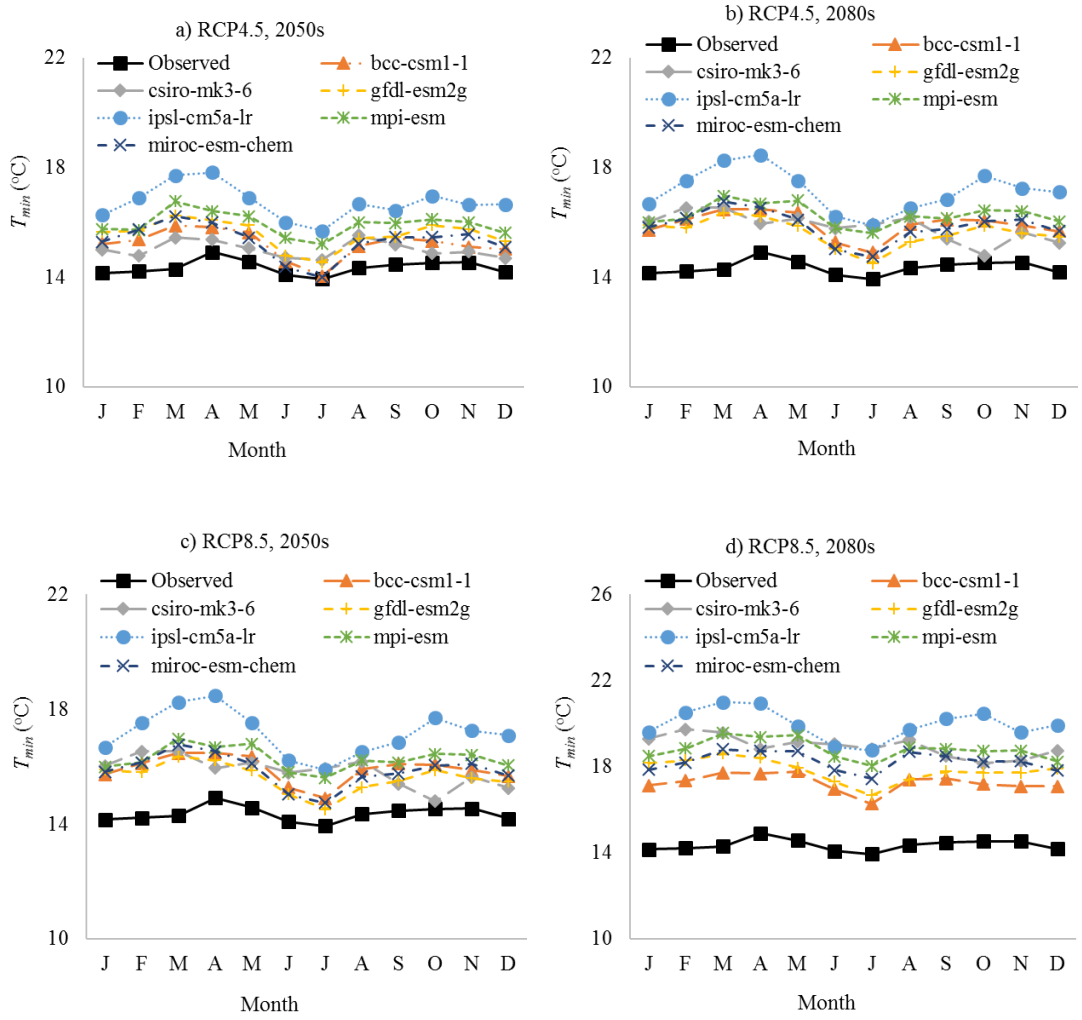

Figure 4-7: Projected change in T_{min}

4.4 Rainfall runoff model

4.4.1 Calibration and validation of AWBM

Figure 4.8 shows calibrated and validated flows for periods 1956- 2002 using AWBM. Calibration was done with the data from 1956 to 1989 whereas validation was done for the years 1990- 2002. The optimal parameters used for calibration are shown in

(Table. 4.1). The NSE for calibration and validation was 0.454 and 0.451, respectively. This shows a good performance of AWBM for reproduction of the daily flow series in Rwizi catchment. Thus, indicating that the model could be satisfactorily applied for climate change impact investigation.

Table 4.1: Optimal Parameters of AWBM

S/No	**Parameter description**	**Unit**	**Parameter values**
1	Partial Area = A1	(—)	0.414
2	Partial Area = A2	(—)	0.386
3	Base Flow Index = BFI	(—)	0.580
4	Capacities = C1	(mm)	0.0
5	Capacities = C2	(mm)	38.0
6	Capacities = C3	(mm)	500.0
7	Baseflow recession constant = K_{base}	(day)	1.000
8	Surface flow recession constant = K_{surf}	(day)	0.970

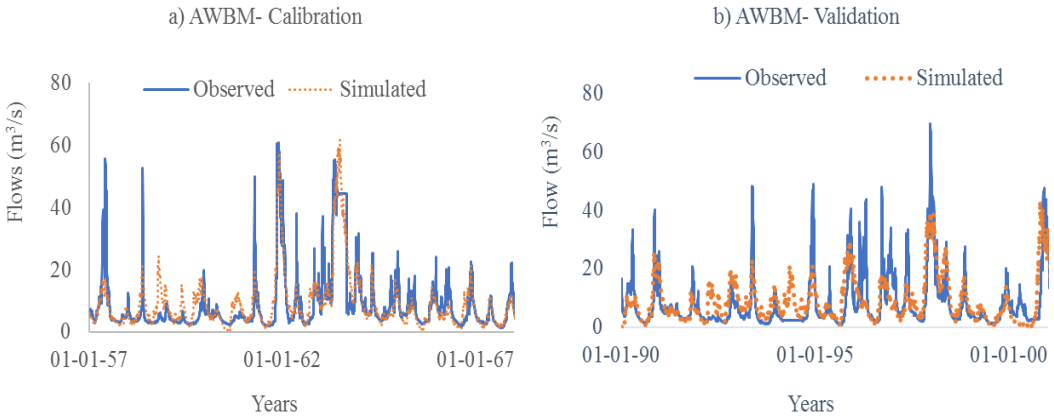

Figure 4-8: Hydrographs of simulated flows using observed data- AWBM

4.4.2 Calibration and validation of HMSV

Figure 4.9 shows calibrated and validated flows for periods 1957- 2002 using HMSV. Calibration was done with the data from 1956 to 1989. The validation was done for the years 1990- 2002. The optimal parameters used for calibration are shown in (Table. 4.2). The NSE for calibration and validation was 0.442 and 0.427, respectively. This shows a good performance of HMSV for reproduction of the daily flow series in Rwizi catchment. Thus, indicating that the model could be satisfactorily applied for climate change impact investigation.

Table 4.2: Optimal parameters of HMSV

S/No	Parameter description	Parameter values
Baseflow sub-model		
1	Initial soil moisture storage (S_0, mm)	158
2	Maximum limit of soil moisture storage deficit (S_{max}, mm)	180

3	Baseflow parameter (α_1)	7.5
4	Baseflow recession constant (t_a, day)	40
Interflow sub-model		
5	Interflow parameter (α_2)	7.3
6	Interflow recession constant (t_b, day)	26
	Overland flow sub-model	
7	Overland flow parameter 1 (α_3)	7
8	Overland flow recession constant 1 (t_u, day)	5
9	Overland flow parameter 2 (c_3)	6
10	Overland flow recession constant 2 (t_v, day)	4

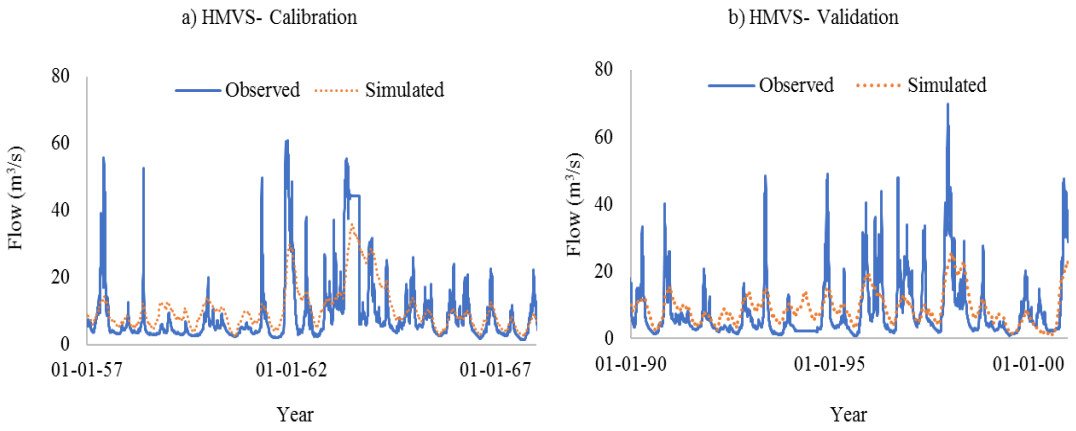

Figure 4-9: Hydrographs of simulated flows using observed data- HMSV

4.5 Future streamflow conditions

4.5.1 Extraction of high flows.

Figure 4.10 shows the projected high flow events for the different GCM runs using AWBM. Figure 4. 10a, b shows the projected flow events in the 2050s and 2080s under scenario RCP4.5. The average projected decrease in high flow events was by about 18.6% (9.497m^3/s) and 15.8% (8.071m^3/s) in the 2050s and 2080s, respectively for 10-year high event under scenario RCP4.5.

Figure 4.10c, d shows projected high flow events under RCP8.5 scenario in the 2050s and 2080s periods. The average projected decrease in high flow events was by about 14.5% (7.393m^3/s) and 3.7% (1.887m^3/s) in the 2050s and 2080s, respectively for 10-year high flow events under scenario RCP8.5. It can be seen from Figure 4.10a, b, c, d that for most GCM runs are below the observed indicating that the flow peaks are projected to decrease the return periods (1-20years).

When assessing impacts of climate change on rainfall in the catchment where the study area falls, Onyutha et al. (2019) considered several GCMs and found that about 50% of the GCMs projected increase (instead of decrease) in rainfall. If rainfall will increase due to the impact of climate change, it means the river flow will also increase. Therefore, the underestimation of future high flows by AWBM could be due to the inaccurately of the model to extract peak flows which might synergistically influence the deficit in the projected flows.

The future flows in River Rwizi are projected to reduce in future. Nyeko- Ogiramoi (2011) projected a decrease in future flows in the same study area over the periods

2050s and 2090s. The perturbation plots (Nyeko-Ogiramoi, 2011) of the flow peak for the most of the GCM runs were below the perturbation value of 1. However, Nyeko-Ogiramoi (2011) used old generation CMIP3 models in the study. In the same region of this study, Kangume (2016) applied SWAT to assess the impact of climate change on the hydroclimatology of Malaba River Catchment, Eastern Ugandan. The study used 3 GCM runs under A1B, A2 and B1 scenarios, and the results projected declines in annual streamflow by about 2.3m3/s in the 2050s under the AIB scenario.

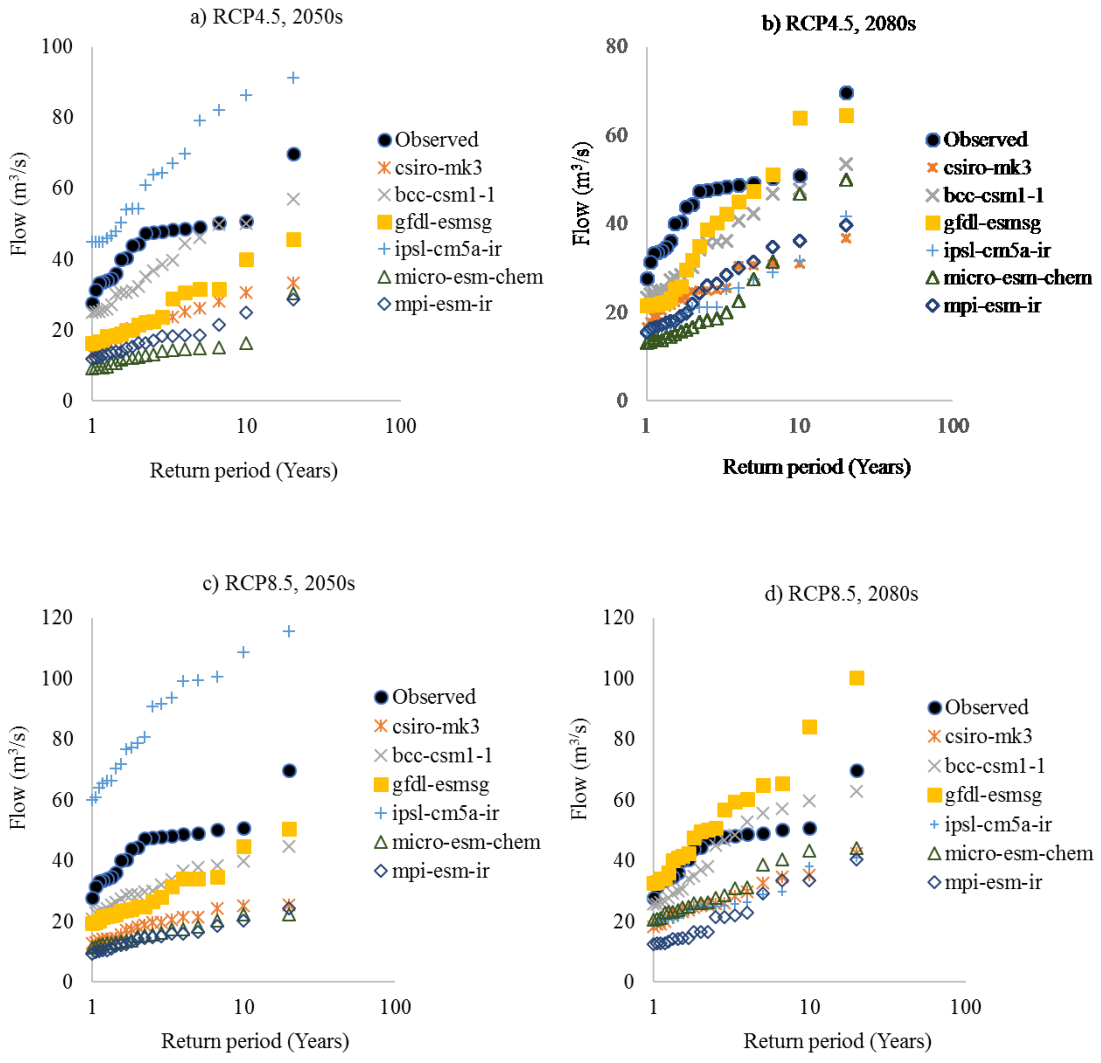

Figure 4-10: Extracted high flow events- AWBM

Figure 4.11 shows the projected high flow events for the different GCM runs using HMSV. Figure 4. 11a, b shows the projected flow events in the 2050s and 2080s under scenario RCP4.5. The mean projected increase in high flow events was 23.7% (5.395m^3/s) and 18.2% (4.138m^3/s) in the 2050s and 2080s, respectively for 10-year high event under scenario RCP4.5.

It can be seen (Figure 4.11a, b) that the projected flows of the 2080s are less compared to the 2050s. The flow deficit can be explained by the fact that temperature was projected to increase which in turn results in an increase of PET during the 2080s under the RCP4.5 scenario.

Figure 4.11c, d shows projected high flow events under RCP8.5 scenario in the 2050s and 2080s periods. The mean projected increase in high flow events was by about 31.2% (7.090m^3/s) and 59.1% (13.434m^3/s) in the 2050s and 2080s, respectively for 10-year high flow events under scenario RCP8.5. It can be seen from Figure 4.9a, b, c, d that the change under the RCP8.5 and RCP4.5 is consistent.

It can be seen that the flows in the 2050s are deficient compared to the flows in the 2080s. The flow deficit can be explained by the decrease in the projected rainfall amounts combined with the increase of PET during the 2080s under the RCP8.5 scenario.

The results of this study agree with Onyutha et al. (2019) who projected increase in rainfall that will result in increase in the river flow. This is attributed to the capacity of HMSV model to extract peak flows.

Generally, the result based on the HMSV are in contrast to those obtained using the AWBM. The main reason for this could the difference in the model structures. Furthermore, it could also be thought of in terms the capacity of the models to capture the extreme events. Here, the HMSV is particularly tailored toward capturing extreme events something which might not be the case with the AWBM. This, therefore, indicates that the use of a particular hydrological model in climate change impact investigation can lead to bias in the results. The question would be which model results to use to support policy regarding adaptation measures. To even out the influence due to the selection of a particular model on the findings, the best practice would be to make use of the results from both hydrological models.

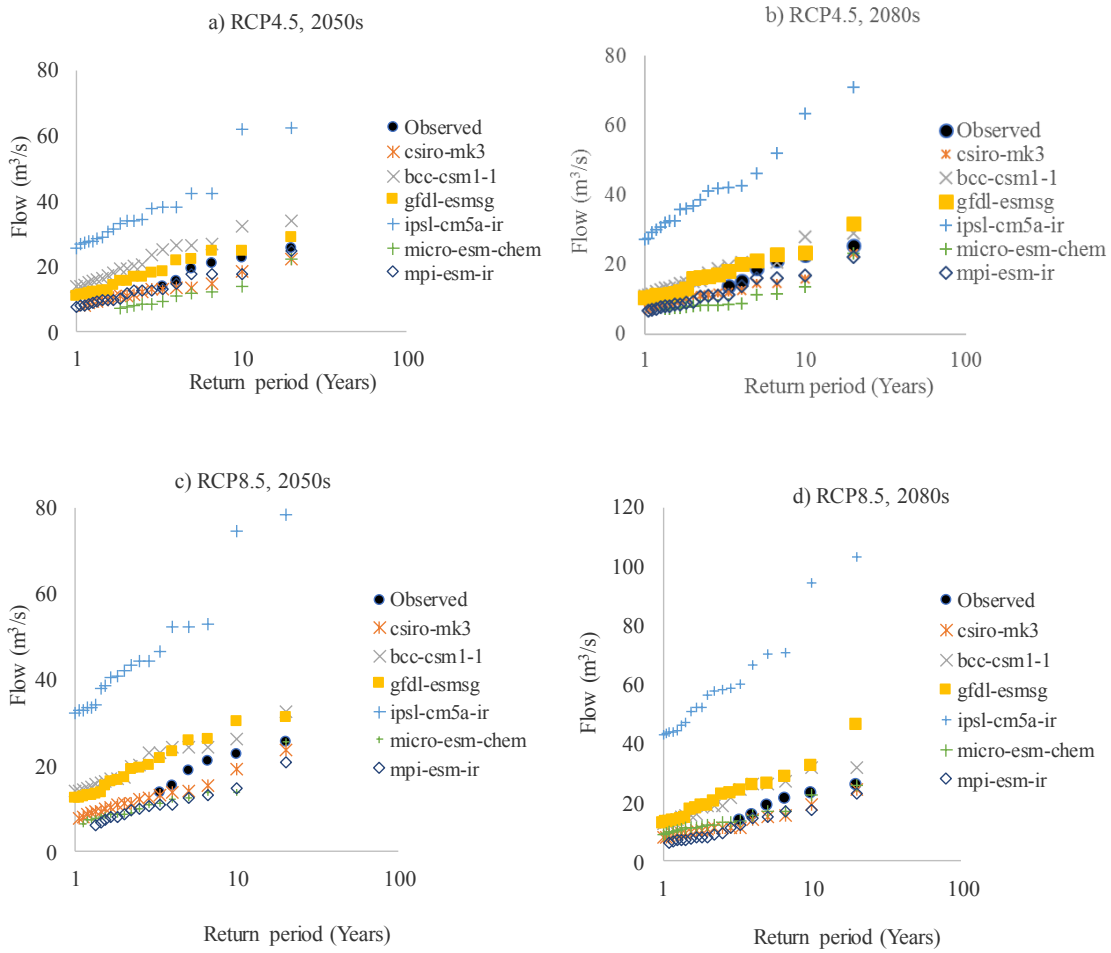

Figure 4-11: Extracted high flow events- HMSV

4.5.2 Extraction of low flow quantiles

Figure 4.12 shows the projected low flows events for the different GCM runs using AWBM. Figure 4. 10a, b shows the projected low flows events in 2050s and 2080s under the RCP4.5. For the 10- year low flow quantile, the average increase in low flow events was by about 11.1% (0.093m^3/s) in the 2050s (Figure 4.12a). Whereas in the 2080s, low flow event was projected to decrease by about 0.3% (0.003m^3/s) for 10-year low flow quantile under the RCP4.5 (Figure 4.12b).

Figure 4.12c, d shows the projected low flows under the RCP8.5 in the 2050s and 2080s. The average increase in low flows was on 16.3% (0.136m^3/s) in the 2050s. For the 2080s, the low flow events are projected to reduce by about 2.7% (0.022 m^3/s) for ten 10-year flow quantile under scenario RCP8.5.

Based on the results, it is noticeable that all GCM runs project low flow quantiles to decrease with increase in return period (Figure 4. 12a, b). This indicates dry conditions in the 2050s. This is attributed to low projected future precipitation as compared to the 2080s. For the 2080s, low flow quantiles anticipated to increase for some GCM runs.

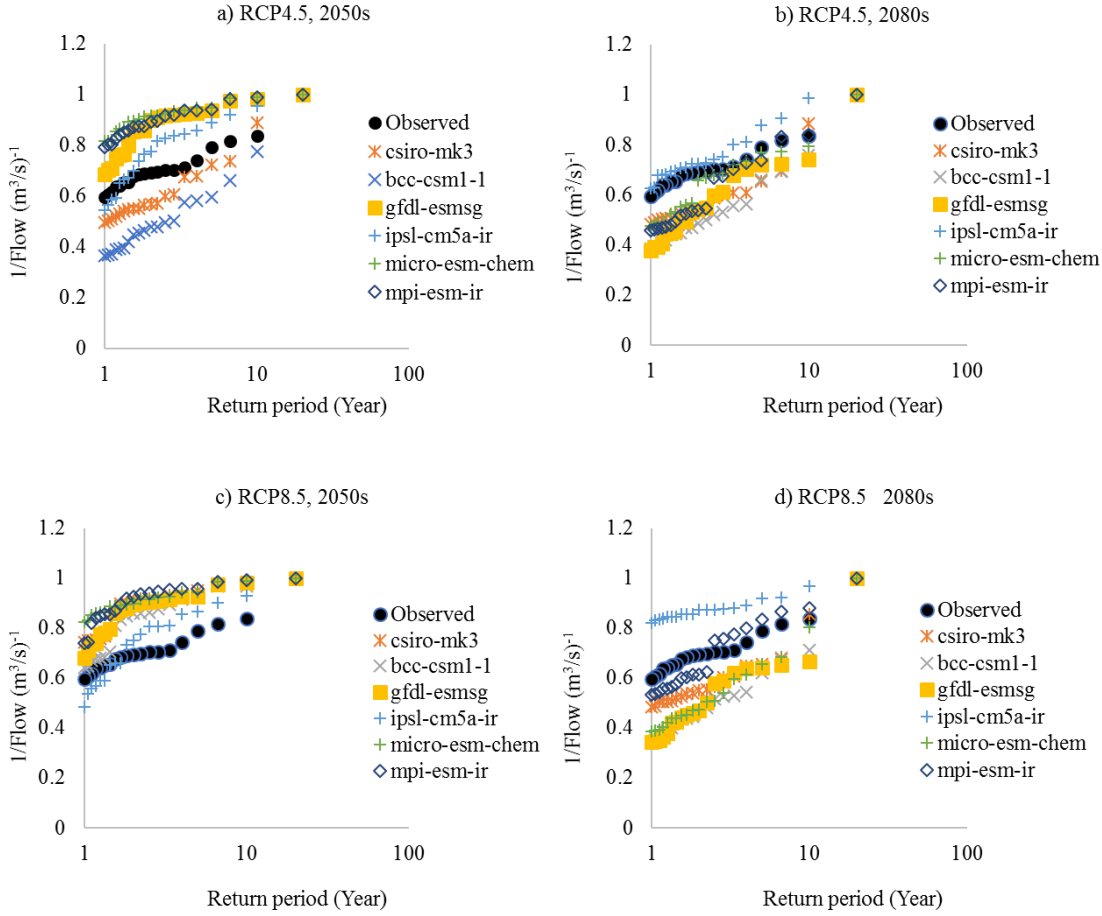

Figure 4-12: Extracted Low flow events- AWBM

Figure 4.13. shows the projected low flows events for the different GCM runs using HMSV model. Figure 4. 13a, b shows the projected low flows events in 2050s and 2080s under the RCP4.5. For the 10- year low flow quantile, the average increase in low flow events was by about 34.5% (0.262m^3/s) and 48.9% (0.372m^3/s) in the 2050s and 2080s, respectively for 10-year low flow quantile under the RCP4.5.

Figure 4.13c, d shows the projected low flows events under the RCP8.5 in the 2050s and 2080s. The average increase in low flows was 22.9% (0.174m^3/s) and 24.9% (0.189m^3/s) in the 2050s and 2080s, respectively for ten 10-year flow quantile under scenario RCP8.5.

It can be seen that all GCM runs project increase of low flow quantile with increase in return period except ipsl-cm5a-ir model (Figure 4.13). This is attributed to the capacity of HMSV model in simulating low flow events.

Overall, the result of low flow quantiles based on the HMSV are divergent to those obtained using the AWBM. The foremost reason for this could be the difference in the model structures. HMSV model has capacity to capture the low flow events something which might not be the case with the AWBM. As stated before, the use of a particular hydrological model in climate change impact investigation can lead to bias in the results. The best practice would be to make use of the results from both hydrological models to even out the influence due to the selection of a particular model on the findings.

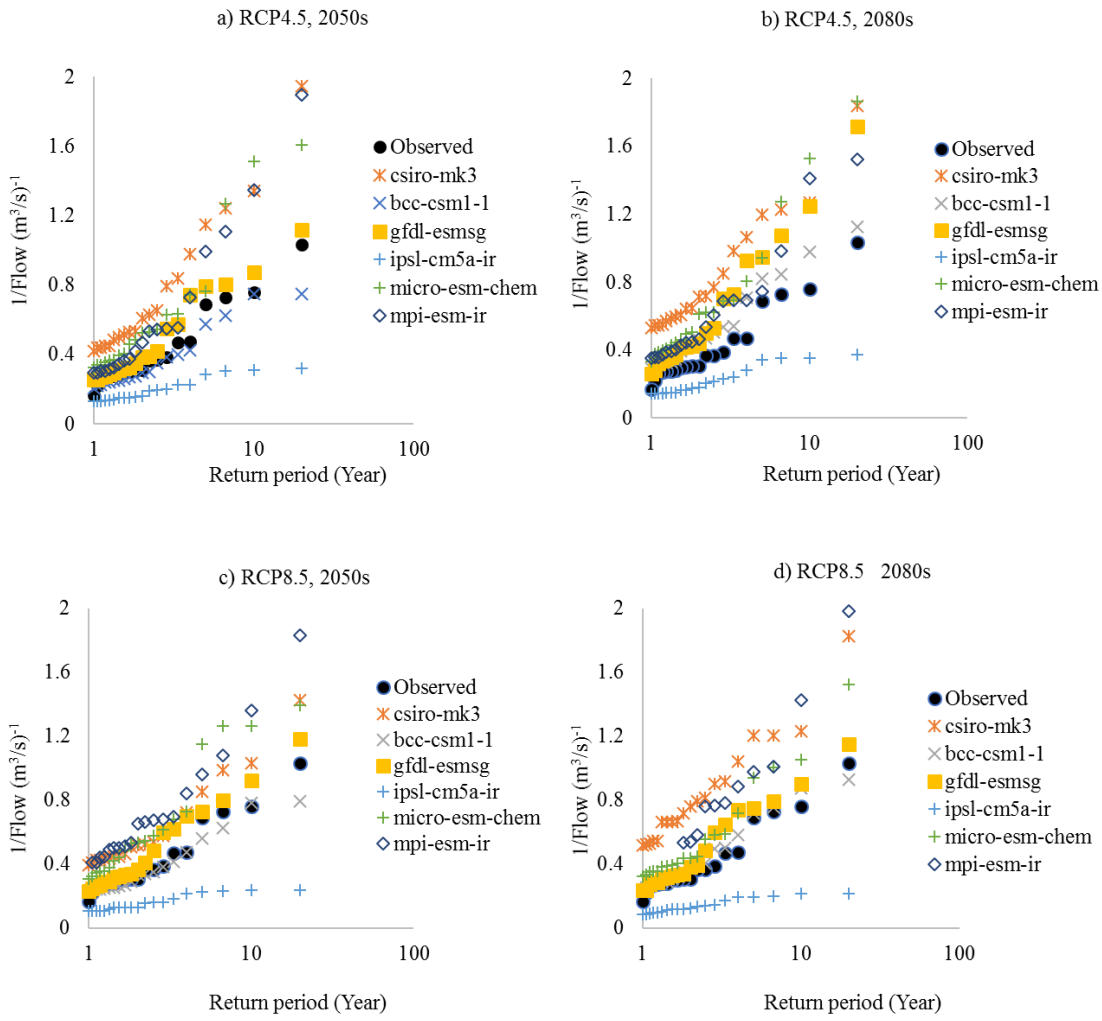

Figure 4-13: Extracted Low flow events- HMSV

CHAPTER FIVE: CONCLUSIONS AND RECOMMENDATIONS

5.1. Conclusions

The trend analysis exhibited that precipitation will increase. The PET showed a decreasing trend. However, the trends in both precipitation and PET were mainly insignificant.

The GCMs show wide range of ability to simulate precipitation, T_{max} and T_{min}. In addition, clear variation was observed on the obtained climate change signal according to the GCM and emission scenario considered.

Precipitation of the 2050s and 2080s will be higher than that of historical period (1956-2002). Under the RCP4.5, the precipitation is projected to increase by 14% and 19% for 2050s and 2080s, respectively. However, for the RCP8.5, the precipitation is projected to increase by 18% and 35% for the 2050s and 2080s, respectively. The projected increase in T_{max} in the 2050s and 2080s was 1% and 2% respectively for RCP4.5 and 4% and 10% for the RCP8.5. Whereas T_{min} is projected to increase in the 2050s and 2080s by about 8.7% and 12.2%, respectively under the RCP4.5 and 14.6 % and 28.3% for the RCP8.5.

The findings from the two lumped conceptual hydrological models illustrate that the range of percentage change is in contrast order of magnitude and sign. Therefore, the hydrological uncertainties have influence on the future climate change results compared to the uncertainty in the GCM results.

The performance of conceptual models in terms of NSE for calibration and validation was 0.454 and 0.451, respectively for AWBM. and 0.442 and 0.427, respectively for

HMSV model. This shows that the conceptual models were satisfactory for application for climate change investigation.

Considering the impact results based on the GCM runs used, HMSV model shows increasing flow extremes as opposed to AWBM which shows decreasing flow extremes.

AWBM projected high flow events to reduce by about 18.6% and 15.8% in the 2050s and 2080s, respectively for 10-year high event under scenario RCP4.5. For the RCP8.5, the high events are projected to reduce by about 14.5% and 3.7% in the 2050s and 2080s, respectively for 10-year high flow events. Whereas, HMSV projected high flows to increase by about 23.7% and 18.2% in the 2050s and 2080s, respectively for 10-year high event under scenario RCP4.5. For the RCP8.5, high flows are projected to increase by about 31.2% (7.090m3/s) and 59.1% (13.434m3/s) in the 2050s and 2080s, respectively for 10-year high flow events under scenario RCP8.5.

The low flow quantiles are projected to reduce with increase in return period under AWBM. However, more decrease in low flows were obtained in the 2050s. Whereas, for HMSV, the low flow quantiles are projected to increase in both periods in both periods.

Overall, the range of projections obtained in this study is much wider than in previous studies within the upper Rwizi Catchment. This is due to the new generation of CMIP5 models used and the hydrological models. These impacts of climate change on the streamflow indicates the need for adequate planning of the relevant and appropriate adaption measures at the catchment scale.

5.2. Recommendations

i) This study ignored the response of changing land use on the hydrology of the catchment. Therefore, a research on hydrological impact assessment using physical based hydrological models which considers other factors such as land use is proposed.

ii) Future study on the water availability and allocation to different actors in the Rwizi catchment is proposed. The simulated flows in this study did not take into account the current or growing water demands.

iii) In addition, the use of Regional Climate Models (RCMs) would be better for hydrological impact studies as their spatial resolution is less coarse than the GCMs. RCMs would indeed enable better coverage of topographical variations across the catchment.

REFERENCES

AKURUT, M., WILLEMS, P. and NIWAGABA, B. C. (2014) Potential impacts of climate change on precipitation over Lake Victoria, East Africa, in the 21st Century. *Water,* 6 (9), pp. 2634-2659.

ALAMOU, A. E., OBADA, E. and AFOUDA, A. (2017) Assessment of future water resources availability under climate change scenarios in the Mékrou basin, Benin. *Hydrology,* 4 (4), p. 51. https://doi.org/10.3390/hydrology4040051.

AGUILAR, E. et al. (2005) Changes in precipitation and temperature extremes in Central America and northern South America, 1961–2003. *Journal of Geophysical Research*, 110 (D23). https://doi.org/10.1029/2005JD006119.

ANDERSON, L. R. (1941) Distribution of the serial correlation coefficients. *Annals of Mathematical Statistics*, 8 (1), pp. 1-13.

ATWONGYEIRE, D., SSEKANDI, J., TUMWESIGYE, W., NDIHIZIWE, D. and NAGAWA, G. (2018) Land use practices in the rural and urban sub catchments of River Rwizi, western-Uganda; Their effect on its ecological characteristics. *International Journal of Energy and Environmental Science*, 3 (2), pp. 45-50.

BEDIENT, B. P. and HUBER, C. W. (1992) *Hydrology and floodplain analysis.* 2rd ed. Reading, Mass: Addison-Wesley.

BEVEN, J. K. (1989) Changing ideas in hydrology- The case of physically based models. *Journal of Hydrology*, 105 (1), pp. 157-172.

BEVEN, J. K. and KIRKBY, J. M. (1979) A physically based variable contributing area model of basin hydrology. *Modern Hydrology*, 24 (1), pp. 43-69.

BEVEN, J. K., KIRKBY, J. M., SCHOFIELD, N. and TAGG, A. F. (1984) Testing a physically based flood forecasting model (TOPMODEL) for three UK catchments. *Journal of Hydrology*, 69 (1), pp. 119-143.

BOUGHTON, W. (2009) Selecting parameter values for the AWBM daily rainfall-runoff model for use on ungauged catchments. *Journal of Hydrologic Engineering*, 14 (12), pp. 1343–1350.

BOUGHTON, W. (2004). The Australian Water Balance Model. *Environmental Modelling & Software*, 19 (10), pp. 943-956.

BRAZIL, E. L. and HUDLOW, D. M. (1981) Calibration procedures used with the National Weather Service River Forecast System. In: Water and Related Land Resource Systems, New York. pp. 457-. 466.

CHIEW, F. H. S. and MCMAHON, A. T. (1991) Improved modelling of the groundwater processes in HYDROLOG. In: *Proceedings of the 20th hydrology and water resources Symposium, Institute of Engineers Australia.* pp. 492-497.

DANIELS, A. E. MORRISON, J. F, JOYCE, A. L., CROOKSTON, L. N., CHEN, C. S. and MCNULLY, G. S. (2012) General Technical Report. *Climate Projections FAQ*. Department of Agriculture, Forest Service, Rocky Mountain Research Station: Fort Collins, CO, USA, 2012; pp. 1–32.

DESSU, B. S. and MELESSE, A. M. (2012) Impact and uncertainties of climate change on the hydrology of the Mara River basin, Kenya/Tanzania. *Hydrological Processes*. 27 (20), pp. 2973-2986.

DIBIKE, B. Y. and COULIBALY, P. (2005) Hydrologic impact of climate change in the Saguenay watershed: Comparison of downscaling methods and hydrologic models. *Journal of Hydrology*, 307 (1-4), pp. 145-163.

EGERU, A., BARASA, B., NAMPIJJA, J., SIYA, A., MAKOOMA, M. T. and MAJALIWA, G. J. M. (2019) Past, present and future climate trends under varied RCP for a sub-humid region in Uganda, 7 (3), p.35. https://doi.org/10.3390/cli7030035.

FRICKO, O., HAVLIK, P., ROGELJ, J., KLIMONT, Z. and GUSTI, M. (2017) The marker quantification of the Shared Socioeconomic Pathway 2: A middle-of-the-road scenario for the 21st century. *Global Environmental Change,* 42, pp. 251–267. https://doi.org/10.1016/j.gloenvcha.2016.06.004.

HALIMATOU, T., KALIFA, T. and KYEI-BAFFOUR, N. (2017) Assessment of changing trends of daily precipitation and temperature extremes in Bamako and Ségou in Mali from 1961- 2014. *Weather and climate extremes*, 18, pp. 8-16.

HEPWORTH, N. and GOULDEN, M. (2008) Climate change in Uganda: Understanding the implications and appraising the response. https://reliefweb.int/report/uganda/climate-change-uganda-understanding-implications-and-appraising-response. [Accessed on 8/7/2019].

HARGREAVES, G. H. and ALLEN, G. R. (2003) History and evaluation of Hargreaves evapotranspiration equation. *Irrigation and Drainage Engineering*, 129 (1), pp. 53–63.

HUBER, W. and ROESNER, L. (2012) The history and evolution of the EPA SWMM. In: *Fifty years of watershed modelling - past, present and future*. http://dc.engconfintl.org/watershed/29. [Accessed on 8/7/2019].

IPCC, 2007: Climate Change 2007: *Synthesis Report. Contribution of Working Groups I, II and III to the Fourth Assessment Report of the Intergovernmental Panel on Climate Change*, Geneva, Switzerland. P. 104

IPCC (2001) Climate change 2001: *The scientific basis. Contribution of working group 1 to the third assessment report of the IPCC*. https://doi.org/10.1002/joc.763.

KANGUME, C. (2016) *Assessing the impacts of climate change on streamflow in Malaba river catchment, Uganda*. Dissertation (MSc) University of Dar es Salaam.

KENDALL, G. M. (1975) *Rank Correlation Methods*. 4th ed. London: Charles Griffin.

KIZZA, M., RHODE, A., XU, C., NTALE, H., K. and HALLDIN, S. (2009) Temporal rainfall variability in the Lake Victoria basin in East Africa during the twentieth century. *Theoretical Applied Climatology*, 98, pp. 119–135.

LAIO, F., DI-BALDASSARRE, G. and MONTANARI, A. (2009) Model selection techniques for the frequency analysis of hydrological extremes. *Water Resources Research*, 45 (7). https://doi.org/10.1029/2007WR006666.

LANG, M., OUARDA, B. J. M. T. and BOBÉE, B. (1999) Towards operational guidelines for over-threshold modelling. *Journal of Hydrology*, 225 (3-4), pp. 103–117.

LANGBEIN, W. B. (1949) Annual floods and the partial-duration flood series. *Transactions American Geophysical Union*, 30 (6), pp. 879–881.

LEHMANN, E. L. (1975) *Nonparametrics, statistical methods based on ranks*. San Francisco, CA, USA: Holden-Day Inc.

MAJALIWA. J. G. M., TENYWA. M. M., BAMANYA. D., MAJUGU W., ISABIRYE P., NANDOZI, C., NAMPIJJA, J., MUSINGUZI, P, NIMUSIIMA, A., LUSWATA, K. C, RAO, C. K. P., BONABANA J., BAGAMBA, F., SEBULIBA, E., AZANGA, E. and SRIDHER G. (2015) Characterization of historical seasonal and annual rainfall and temperature trends in selected climatological homogenous rainfall zones of Uganda. *Global Journal of Science Frontier Research*, 15 (4), pp. 21-40.

MANN, B. H. (1945) Non-Parametric Tests against Trend. *Econometrica*, 13 (3), pp. 245-259.

MBAYE, L. M. (2017) *Assessment of climate change impacts on water resources in the Senegal river basin at Bakel*. Dissertation (PhD), University of Abomey – Calavi.

MCSWEENEY, C., NEW, M. and LIZCANO, G. (2008) The United Nations Development Programme (UNDP): Climate change country profiles, Uganda. http://countryprofiles.geog.ox.ac.uk/index.html. [Accessed on 30/07/2019].

MCSWEENEY, C., LIZCANO, G., NEW, M. and LU, X. (2010) The UNDP Climate Change Country Profiles: Improving the accessibility of observed and projected

climate information for studies of climate change in developing countries. *Bulletin of the American Meteorological Society*, 91 (2), pp. 157-166.

MWE (2018) Uganda National Climate Change Policy (Summary Version). Transformation through climate change mitigation and adaptation. Climate change department, MWE, Entebbe, Uganda.

MWE (2011) The declining trends of water resources in Uganda: A case study of River Ruizi, Lake Wamala, Lake Victoria Catchments and representative groundwater monitoring stations. Water resources monitoring and assessment division, department of monitoring and assessment, Directorate of water resources management MWE, Entebbe, Uganda.

NASH, E. J. and SUTCLIFFE, J. V. (1970) River flow forecasting through conceptual models' part I - A discussion of principles. *Journal of Hydrology*, 10 (3), pp. 282-290.

NAVARRO-RACINES, C. E., TARAPUES-MONTENEGRO, J. E. and RAMÍREZ-VILLEGAS, J. A. (2015) Bias-correction in the CCAFS-Climate Portal: *A description of methodologies. Decision and Policy Analysis (DAPA) research area*. Cali, Colombia.

NSUBUGA, F. N. W., NAMUTEBI, E. N. and NSUBUGA., M. S. (2014) Water resources of Uganda: An assessment and review. *Water Resource and Protection*, 6 (6), pp. 1297-1315.

NSUBUGA, F. N. W., OLWOCH, J. M. and RAUTENBACH, C. J. W. (2011) Climatic Trends at Namulonge in Uganda: 1947-2009. *Journal of Geography and Geology*, 3 (1), pp. 119-131.

NYEKO-OGIRAMOI, P., WILLEMS, P., and NGIRANE-KATASHAYA, G. (2013) Trend and variability in observed hydrometeorological extremes in the Lake Victoria basin. *Journal of Hydrology*, 489, pp. 56-73.

NYEKO-OGIRAMOI, P., WILLEMS, P., NGIRANE-KATASHAYA, G., and NTEGEKA, V. (2012) Climate models. In: DRUYAN, L. (ed.) *Nonparametric statistical downscaling of precipitation from global climate models.* Slavka Krautzeka: InTech Europe, pp. 109–136.

NYEKO-OGIRAMOI, P. (2011) *Climate change impacts on hydrological extremes and water resources in Lake Victoria catchments, upper Nile basin*. Dissertation (PhD), KU Leuven.

NYEKO-OGIRAMOI, P., NGIRANE-KATASHAYA, G., WILLEMS, P., and NTEGEKA. V. (2010) Evaluation and inter-comparison of GCM's performance over Katonga and Ruizi catchments in Lake Victoria basin. *Physics and Chemistry of the Earth*, 35 (13-14), pp. 618-633.

O'CONNELL, E. P, NASH, E. J. and FARRELL, J. P. (1970). River flow forecasting through conceptual models Part I, a discussion of principles. *Journal of Hydrology*, 10, pp. 317-329.

OJOK, W., WASSWA, J. and NTAMBI, E. (2017) Assessment of seasonal variation in water quality in river Rwizi using multivariate statistical techniques, Mbarara municipality, Uganda. *Water Resource and Protection*, 9 (1), pp. 83-97.

OMONDI, A. P et al. (2013) Changes in temperature and precipitation extremes over the Greater Horn of Africa region from 1961 to 2010. *International Journal of Climatology,* 34 (4), pp. 1262-1277.

ONGOMA, V., CHENA, B. H. and CHUJIE, G. (2017) Projected changes in mean rainfall and temperature over East Africa based on CMIP5 models. *International Journal of Climatology,* 38 (3), pp. 1375–1392.

ONYUTHA, C. (2019) Hydrological model supported by a step-wise calibration against sub-flows and validation of extreme flow events. *Water*, 11 (3), p. 244. https://doi.org/10.3390/w11020244.

ONYUTHA, C., TABARI, H., RUTKOWSKA, A., NYEKO-OGIRAMOI, P. and WILLEMS, P. (2019) Comparison of different statistical downscaling methods for climate change rainfall projections over the Lake Victoria basin considering CMIP3 and CMIP5. *Journal of hydro-environment research,* 12, pp. 31-45.

ONYUTHA, C. (2018) Trends and variability in African long-term precipitation. *Stochastic Environmental Research and Risk Assessment,* 32 (9), pp. 2721-2739.

ONYUTHA, C. (2017) On rigorous drought assessment using daily time scale: Non-Stationary Frequency Analyses, revisited concepts, and a new method to yield non-parametric indices. *Hydrology,* 4(4), p. 48. https://doi.org/10.3390/hydrology4040048.

ONYUTHA, C. (2016a) Geospatial trends and decadal anomalies in extreme rainfall over Uganda, East Africa. *Advances in Meteorology*, 2016, pp. 1–15.

ONYUTHA, C. (2016b) Influence of hydrological model selection on simulation of moderate and extreme flow events: A case study of the Blue Nile basin. *Advances in Meteorology*, 2016.

ONYUTHA, C. (2016c) Identification of sub-trends from hydro-meteorological series. *Stochastic environmental research and risk assessment*, 30 (1), pp. 189-205.

ONYUTHA, C. (2016d) Statistical uncertainty in hydrometeorological trend analyses. Advances in Meteorology, 2016. http://dx.doi.org/10.1155/2016/8701617.

ONYUTHA, C. and WILLEMS, P. (2015) Uncertainty in calibrating generalised Pareto distribution to rainfall extremes in Lake Victoria Basin. *Hydrology Research*, 46 (3), pp. 356–376.

PORTER, J. W. (1972) *The synthesis of continuous streamflow from climatic data by modelling with a digital computer*. Dissertation (PhD), Monash University.

PORTER, J. W. and MCMAHON, A. T. (1975) Application of a catchment model in south eastern Australia. *Journal of Hydrology*, 24 (1-2), pp. 121–134.

RAMIREZ-VILLEGAS, J., CHALLINOR, A. J. THORNTON, K. P. and JARVIS, A. (2013) Implications of regional improvement in global climate models for agricultural impact research. *Environmental Research Letters*, 8 (2), pp. 1-12.

RIAHI, K., VUUREN, D. P., KRIEGLER, E., EDMONDS, J., O'NEILL, B., FUJIMORI, S., BAUER, N. and CALVIN, K. (2017) The shared socioeconomic pathways and their energy, land use, and greenhouse gas emissions implications: An overview. *Global Environmental Change,* 42, pp. 153-168. DOI: 10.1016/j.gloenvcha.2016.05.009.

PRASADA, P. R. V. V. and ADDISU, L. S. (2013) Trend analysis and adaptation strategies of climate change in north central Ethiopia. *International Journal of Agricultural Science and Research*, 3 (1), pp. 253-262.

SALAS, J. D., DELLEUR, J. W., YEVJEVICH, V. and LANE, W. L. (1980) *Applied modelling of hydrologic time series*. Littleton: Water Resources Publications.

SAZIB, N. S. (2016) *Physically based modelling of the impacts of climate change on streamflow regime*. Dissertation (PhD), Utah State University Logan, Utah.

SEN, K. P. (1968) Estimates of the Regression Coefficient Based on Kendall's Tau. *Journal of the American Statistical Association*, 63 (324), pp. 1379-1389.

SHEPARD, D. (1968) A two-dimensional interpolation function for irregularly-spaced data. Proceedings of the 1968 ACM national conference, New York. http://dx.doi.org/10.1145/800186.810616.

SMITH, R. L. (1985) Threshold Methods for Sample Extremes. *In Statistical Extremes and Applications.* Netherland: Dordrecht, 131, pp. 623–638.

SNEYERS, R. (1990) *On the statistical analysis of series of observations*; Technical Note no. 143, WMO no. 415; Secretariat of the World Meteorological Organization: Geneva, Switzerland.

SOCOLOW, H. R. and PACALA, S. W. (2006) A plan to keep carbon in check. *Scientific American*, 295 (3), pp. 50–57.

SONGA. P., RUMOHR. J. and MUSOTA. R. (2015) A shared water risk assessment for a vulnerable river basin: River Rwizi in Uganda. 197, pp. 213-224. DOI: 10.2495/RM150191.

SPEARMAN, C. (1987) The Proof and Measurement of Association between Two Things. The American Journal of Psychology, 100 (3-4), pp. 441-471.

SUGAWARA, M. and FUNIYUKI, M. (1956) A method of revision of the river discharge by means of a rainfall model. Collection of research papers about forecasting hydrologic variables, pp. 14-18.

TAYLOR. T., MARKANDYA. A., DROOGERS. P. and RUGUMAYO, P. (2014) Economic assessment of the impacts of climate change in Uganda: Data water sector report, November.

THEIL, H. (1950) *A rank-invariant method of linear and polynomial regression analysis*. Amsterdam, Netherlands: Economic Research Institute.

TRENBERTH, K. E., et al., (2007) Observations: Surface and atmospheric climate change. In: climate change 2007. The physical science basis. Contribution of WG 1 to the Fourth Assessment Report of the IPCC. pp. 235–336.

TRZASKA, S. and SCHNARR, E. (2014) A review of Downscaling Methods for Climate Change Projections: African and Latin American Resilience to Climate Change (ARCC). http://www.ciesin.org/documents/Downscaling_CLEARED_000.pdf. [Accessed on 11/8/2019].

APPENDICES

Extracted high flows (m^3/s)- AWBM

RCP4.5, 2050s						
Observed	csiro-mk3	bcc-csm1-1	gfdl-esmsg	ipsl-cm5a-ir	micro-esm-chem	mpi-esm-ir
69.739	33.452	57.062	45.795	91.386	30.410	28.720
50.928	30.718	50.124	40.052	86.423	16.373	24.894
50.351	28.301	49.883	31.588	82.225	15.252	21.432
49.083	26.350	46.129	31.543	79.184	14.776	18.673
48.751	25.203	44.502	30.609	69.914	14.619	18.554
48.304	23.803	39.839	29.043	67.081	14.328	18.388
47.931	23.303	38.545	23.869	64.522	14.240	18.376
47.552	22.748	36.938	22.639	64.002	13.072	17.031
47.362	21.890	35.141	22.166	60.935	12.890	16.420
44.451	21.678	32.294	21.534	54.368	12.346	16.397
43.898	20.640	31.240	20.186	54.272	12.301	15.278
40.556	19.942	30.734	19.954	54.067	12.162	14.987
40.118	18.281	30.696	19.080	50.387	11.618	13.913
36.093	17.488	30.268	18.675	47.946	10.719	13.827
34.722	17.017	27.165	18.458	46.784	10.642	13.573
33.992	16.963	25.920	18.328	45.844	9.659	13.217
33.573	16.877	25.670	16.923	45.018	9.553	13.034
33.355	14.785	25.300	16.911	44.959	9.458	12.341
31.491	14.404	25.199	16.456	44.922	9.411	12.275
27.751	13.391	25.118	16.339	44.908	9.155	11.871
RCP4.5,2080s						
Observed	csiro-mk3	bcc-csm1-1	gfdl-esmsg	ipsl-cm5a-ir	micro-esm-chem	mpi-esm-ir
69.739	36.723	53.483	64.476	41.661	49.958	39.677
50.928	30.990	47.740	63.880	31.659	46.796	36.079
50.351	30.766	46.886	51.073	29.045	31.470	34.715
49.083	30.604	42.358	47.406	27.523	27.440	31.409
48.751	30.515	40.665	44.979	25.432	22.592	29.967
48.304	25.421	36.238	42.316	25.230	20.066	28.512
47.931	25.164	35.881	40.225	21.228	18.608	26.436
47.552	24.932	35.858	38.713	21.205	18.300	26.196
47.362	24.871	34.215	35.064	21.140	17.771	24.246
44.451	24.664	30.278	31.793	20.919	16.558	22.044
43.898	23.549	29.386	29.704	20.043	16.105	19.815
40.556	22.962	28.433	25.851	19.409	15.583	19.203
40.118	22.333	27.933	25.377	17.631	15.073	18.116

36.093	21.844	27.384	23.100	17.051	14.437	18.067
34.722	21.399	25.055	22.387	16.458	14.392	17.568
33.992	20.360	25.015	22.177	16.448	13.707	17.194
33.573	19.289	24.934	21.790	16.249	13.694	16.876
33.355	19.066	24.409	21.714	15.897	13.608	16.646
31.491	17.752	24.047	21.681	15.822	13.318	16.395
27.751	16.635	23.345	21.588	15.604	13.040	15.489
RCP8.5, 2050s						
Observed	csiro-mk3	bcc-csm1-1	gfdl-esmsg	ipsl-cm5a-ir	micro-esm-chem	mpi-esm-ir
69.739	25.399	44.866	50.518	115.737	22.442	24.343
50.928	25.067	40.013	44.804	108.735	22.396	20.195
50.351	24.178	38.491	34.578	100.652	20.152	18.439
49.083	21.446	37.935	34.242	99.628	18.312	16.644
48.751	21.366	36.831	34.218	99.383	17.458	15.958
48.304	20.513	33.942	31.385	93.661	17.265	15.919
47.931	19.812	32.116	27.941	91.757	16.315	15.069
47.552	19.583	30.150	26.636	90.978	15.772	14.745
47.362	18.837	29.812	24.837	80.915	15.308	14.497
44.451	18.317	29.049	24.761	78.660	15.048	14.246
43.898	17.509	28.899	24.008	77.342	13.647	13.503
40.556	17.175	28.542	23.830	76.637	13.575	12.531
40.118	15.758	27.450	23.470	71.777	13.322	12.341
36.093	14.515	26.342	22.266	70.441	13.069	11.971
34.722	14.371	25.413	21.952	66.424	12.880	11.102
33.992	14.269	24.246	21.865	66.377	12.855	10.382
33.573	14.120	23.322	21.369	65.606	12.502	10.372
33.355	13.780	23.026	20.271	64.118	12.181	10.317
31.491	13.209	22.886	19.659	60.785	11.780	9.969
27.751	12.855	20.781	19.564	60.028	11.413	9.436
RCP8.5, 2080s						
Observed	csiro-mk3	bcc-csm1-1	gfdl-esmsg	ipsl-cm5a-ir	micro-esm-chem	mpi-esm-ir
69.739	42.371	63.012	100.464	41.036	44.331	40.502
50.928	35.327	59.644	84.372	38.050	43.230	33.622
50.351	34.662	57.075	65.492	29.895	40.557	33.491
49.083	32.653	55.626	64.903	29.074	38.806	29.165
48.751	29.842	52.814	60.416	26.444	31.243	22.846
48.304	28.300	48.555	59.434	25.698	31.012	22.083
47.931	26.080	46.853	56.926	25.060	28.770	21.578
47.552	25.650	45.115	50.723	24.954	27.640	21.448
47.362	25.564	38.257	50.156	24.898	26.263	16.681

44.451	25.322	36.920	49.617	24.861	25.985	16.525
43.898	24.717	35.092	47.678	24.506	25.907	16.435
40.556	23.799	34.078	42.505	23.836	24.983	14.548
40.118	23.250	30.687	41.542	22.406	24.526	14.467
36.093	22.965	30.018	41.173	21.142	23.699	14.187
34.722	22.267	29.318	40.119	20.663	23.244	14.140
33.992	21.379	27.708	36.136	20.642	23.221	13.382
33.573	20.027	26.696	34.160	20.314	22.964	12.924
33.355	19.127	26.476	34.114	20.308	21.289	12.852
31.491	19.100	25.702	32.989	19.269	20.983	12.841
27.751	18.274	25.693	32.597	19.159	20.583	12.410

Extracted low flow quantiles (m^3/s)- AWBM

RCP4.5, 2050s						
Observed	csiro-mk3	bcc-csm1-1	gfdl-esmsg	ipsl-cm5a-ir	micro-esm-chem	mpi-esm-ir
1.000	1.000	1.000	1.000	1.000	1.000	1.000
0.837	0.889	0.777	0.981	0.953	0.991	0.989
0.818	0.737	0.662	0.977	0.921	0.987	0.983
0.791	0.722	0.596	0.936	0.889	0.947	0.942
0.742	0.677	0.582	0.927	0.858	0.947	0.936
0.712	0.675	0.577	0.924	0.845	0.936	0.936
0.704	0.608	0.504	0.921	0.837	0.933	0.919
0.704	0.601	0.495	0.916	0.827	0.924	0.917
0.697	0.574	0.478	0.910	0.815	0.915	0.896
0.693	0.570	0.478	0.898	0.774	0.915	0.891
0.689	0.565	0.464	0.860	0.764	0.913	0.877
0.685	0.552	0.455	0.857	0.736	0.902	0.874
0.678	0.551	0.448	0.855	0.701	0.895	0.871
0.655	0.546	0.419	0.800	0.673	0.892	0.859
0.653	0.541	0.395	0.765	0.664	0.865	0.852
0.641	0.529	0.393	0.762	0.652	0.864	0.841
0.639	0.518	0.388	0.747	0.591	0.855	0.829
0.617	0.510	0.371	0.709	0.586	0.821	0.802
0.607	0.504	0.368	0.702	0.564	0.818	0.801
0.595	0.496	0.365	0.687	0.544	0.817	0.793
RCP4.5, 2080s						
Observed	csiro-mk3	bcc-csm1-1	gfdl-esmsg	ipsl-cm5a-ir	micro-esm-chem	mpi-esm-ir
1.000	1.000	1.000	1.000	1.000	1.000	1.000
0.837	0.885	0.759	0.742	0.987	0.792	0.840

0.818	0.695	0.692	0.723	0.904	0.774	0.831
0.791	0.654	0.661	0.721	0.878	0.769	0.738
0.742	0.610	0.564	0.702	0.811	0.734	0.726
0.712	0.607	0.558	0.680	0.800	0.721	0.702
0.704	0.597	0.532	0.613	0.751	0.685	0.674
0.704	0.587	0.521	0.600	0.741	0.680	0.668
0.697	0.550	0.500	0.548	0.727	0.668	0.547
0.693	0.544	0.488	0.541	0.725	0.658	0.540
0.689	0.537	0.469	0.532	0.722	0.566	0.537
0.685	0.530	0.468	0.495	0.711	0.560	0.525
0.678	0.526	0.448	0.492	0.707	0.553	0.517
0.655	0.518	0.445	0.453	0.697	0.530	0.493
0.653	0.507	0.440	0.447	0.693	0.523	0.480
0.641	0.506	0.420	0.444	0.681	0.490	0.473
0.639	0.505	0.411	0.404	0.680	0.489	0.469
0.617	0.500	0.393	0.391	0.679	0.488	0.466
0.607	0.489	0.387	0.391	0.630	0.480	0.463
0.595	0.483	0.386	0.377	0.627	0.477	0.458
RCP8.5, 2050s						
Observed	csiro-mk3	bcc-csm1-1	gfdl-esmsg	ipsl-cm5a-ir	micro-esm-chem	mpi-esm-ir
1.000	1.000	1.000	1.000	1.000	1.000	1.000
0.837	0.979	0.968	0.983	0.930	0.988	0.993
0.818	0.977	0.967	0.974	0.900	0.986	0.986
0.791	0.949	0.922	0.927	0.867	0.945	0.958
0.742	0.933	0.917	0.926	0.857	0.945	0.957
0.712	0.932	0.895	0.916	0.811	0.924	0.955
0.704	0.923	0.878	0.907	0.807	0.924	0.945
0.704	0.920	0.862	0.906	0.806	0.916	0.939
0.697	0.920	0.860	0.900	0.776	0.916	0.937
0.693	0.908	0.860	0.896	0.750	0.898	0.927
0.689	0.903	0.850	0.880	0.732	0.893	0.919
0.685	0.897	0.834	0.872	0.661	0.892	0.893
0.678	0.861	0.809	0.859	0.658	0.887	0.870
0.655	0.855	0.703	0.794	0.651	0.886	0.857
0.653	0.769	0.684	0.781	0.590	0.863	0.855
0.641	0.757	0.679	0.776	0.588	0.863	0.847
0.639	0.754	0.676	0.739	0.567	0.861	0.843
0.617	0.750	0.671	0.737	0.558	0.853	0.820
0.607	0.750	0.649	0.712	0.536	0.831	0.744
0.595	0.742	0.642	0.682	0.484	0.824	0.740
RCP8.5, 2080s						

Observed	csiro-mk3	bcc-csm1-1	gfdl-esmsg	ipsl-cm5a-ir	micro-esm-chem	mpi-esm-ir
1.000	1.000	1.000	1.000	1.000	1.000	1.000
0.837	0.854	0.713	0.667	0.970	0.803	0.880
0.818	0.680	0.674	0.653	0.923	0.683	0.868
0.791	0.655	0.622	0.642	0.918	0.657	0.833
0.742	0.648	0.545	0.639	0.889	0.613	0.799
0.712	0.608	0.530	0.620	0.879	0.596	0.774
0.704	0.605	0.527	0.588	0.877	0.541	0.756
0.704	0.565	0.514	0.577	0.874	0.509	0.749
0.697	0.554	0.481	0.502	0.873	0.504	0.626
0.693	0.550	0.470	0.469	0.872	0.472	0.614
0.689	0.539	0.446	0.458	0.855	0.468	0.612
0.685	0.537	0.440	0.454	0.855	0.454	0.603
0.678	0.526	0.434	0.441	0.854	0.449	0.599
0.655	0.520	0.424	0.425	0.847	0.440	0.575
0.653	0.510	0.398	0.421	0.847	0.437	0.564
0.641	0.505	0.390	0.379	0.846	0.422	0.559
0.639	0.505	0.385	0.364	0.839	0.403	0.559
0.617	0.504	0.364	0.351	0.835	0.393	0.543
0.607	0.487	0.361	0.347	0.830	0.389	0.538
0.595	0.485	0.341	0.345	0.822	0.387	0.534
	0.021	-0.148	-0.203	0.159	-0.040	0.051

Extracted high flows- HMSV model

RCP4.5, 2050s						
Observed	csiro-mk3	bcc-csm1-1	gfdl-esmsg	ipsl-cm5a-ir	micro-esm-chem	mpi-esm-ir
25.516	22.316	34.036	29.036	62.197	22.169	24.583
22.750	18.420	32.333	24.733	61.988	13.774	17.625
21.037	14.435	26.609	24.563	42.098	12.162	17.432
18.998	13.355	26.427	22.198	42.090	11.697	17.391
15.394	13.174	26.408	21.689	38.223	10.723	14.750
13.819	12.986	25.075	18.547	37.851	9.353	12.926
	12.964	23.521	18.015	37.593	8.506	12.678
	11.927	20.249	16.761	34.437	8.144	12.485
	11.096	19.918	16.637	34.054	7.810	12.470
	10.905	19.331	15.429	33.765	7.648	11.562
	10.718	19.278	15.316	33.186	7.048	10.173
	10.545	17.791	14.070	31.179		9.689

	9.969	17.041	12.637	30.401		9.685
	9.495	16.464	12.599	28.662		9.651
	9.103	15.727	12.092	28.300		9.191
	9.098	15.278	11.920	27.697		8.762
	8.568	14.956	11.767	27.671		8.508
	8.060	14.292	11.420	27.045		8.092
		13.875	11.250	26.651		7.746
		13.869	10.730	25.670		7.361
RCP4.5, 2080s						
Observed	csiro-mk3	bcc-csm1-1	gfdl-esmsg	ipsl-cm5a-ir	micro-esm-chem	mpi-esm-ir
25.516	23.080	29.021	31.698	71.069	23.126	25.516
22.750	15.807	28.010	23.413	63.509	13.639	22.750
21.037	14.484	20.702	23.041	52.041	11.461	21.037
18.998	14.461	20.693	21.132	46.290	11.245	18.998
15.394	12.616	20.582	20.043	42.569	8.689	15.394
13.819	11.968	19.693	18.223	42.067	8.411	13.819
	11.702	18.928	17.191	42.024	8.358	
	11.259	17.630	16.726	41.113	8.348	
	11.151	15.315	16.288	38.591	8.313	
	10.945	15.172	15.996	36.757	8.063	
	10.401	14.817	13.175	36.127	7.739	
	9.730	14.502	12.235	35.907	7.604	
	9.472	13.816	11.887	32.603	7.451	
	9.139	13.435	11.540	32.446	7.299	
	8.557	13.346	11.397	31.916	7.261	
	8.022	12.880	11.226	30.800		
	7.988	12.358	11.198	30.050		
	7.966	11.623	10.827	29.382		
	6.978	11.189	10.585	27.598		
		11.157	10.491	27.225		
RCP8.5, 2050s						
Observed	csiro-mk3	bcc-csm1-1	gfdl-esmsg	ipsl-cm5a-ir	micro-esm-chem	mpi-esm-lr
25.516	23.706	32.661	31.401	78.346	25.692	20.738
22.750	19.265	26.325	30.456	74.519	13.704	14.770
21.037	15.424	24.327	26.237	52.867	13.645	13.186
18.998	14.151	24.191	25.869	52.161	12.470	12.404
15.394	13.864	24.173	23.197	52.133	12.240	11.026
13.819	13.033	23.133	21.587	46.509	11.084	10.978
	12.451	23.101	20.025	44.337	10.788	10.571
	12.089	20.070	19.362	44.289	10.087	9.858

	11.310	19.955	19.202	43.482	9.004	9.714
	11.163	17.359	17.149	42.229	8.815	8.762
	10.794	16.942	16.723	40.672	8.777	8.048
	10.311	16.899	16.309	40.636	8.753	8.020
	9.848	16.376	15.387	38.660	8.464	7.268
	9.396	16.050	13.630	38.006	8.148	6.771
	9.259	15.570	13.543	34.252	7.874	6.145
	8.968	14.948	13.263	33.504	7.486	
	8.631	14.882	13.131	33.448	7.291	
	8.081	14.396	12.782	32.975	6.532	
	7.740	14.162	12.651	32.947		
		14.019	12.548	32.339		
RCP8.5, 2080s						
Observed	csiro-mk3	bcc-csm1-1	gfdl-esmsg	ipsl-cm5a-ir	micro-esm-chem	mpi-esm-ir
25.516	24.269	31.647	46.226	103.397	25.547	22.940
22.750	19.102	31.631	32.222	94.253	22.730	17.169
21.037	15.642	27.249	28.486	70.553	16.939	17.010
18.998	14.882	26.389	26.143	70.110	16.749	15.219
15.394	14.193	26.256	25.966	66.756	15.475	14.382
13.819	11.435	24.217	23.795	60.050	13.782	12.365
	11.374	21.389	22.821	58.563	13.249	11.460
	11.158	18.948	22.468	58.048	13.026	9.611
	11.146	18.840	19.967	57.764	12.520	9.106
	11.115	18.560	18.774	56.541	12.259	7.991
	10.435	18.215	18.641	52.267	11.806	7.945
	10.405	15.900	17.711	52.038	11.438	7.933
	10.108	15.734	17.210	50.843	11.221	7.808
	9.566	15.702	14.802	47.137	11.219	7.389
	9.495	14.939	14.117	46.347	11.068	7.289
	9.380	14.193	13.720	44.530	10.510	7.279
	8.822	13.861	13.654	44.057	9.974	6.731
	8.587	13.690	13.241	43.906	9.809	6.381
	8.276	13.348	13.056	43.360	9.625	
	8.000	12.847	12.954	42.833	9.126	

Extracted low flow quantiles (m^3/s)- HMSV model

RCP4.5, 2050s						
Observed	csiro-mk3	bcc-csm1-1	gfdl-esmsg	ipsl-cm5a-ir	micro-esm-chem	mpi-esm-ir
1.033	1.946	0.751	1.119	0.319	1.606	1.895
0.759	1.343	0.747	0.871	0.312	1.510	1.346
0.728	1.241	0.626	0.802	0.307	1.265	1.107
0.690	1.149	0.575	0.792	0.285	0.766	0.994
0.472	0.981	0.426	0.743	0.228	0.745	0.729
0.471	0.836	0.399	0.573	0.226	0.637	0.557
0.387	0.792	0.385	0.550	0.199	0.630	0.551
0.368	0.652	0.351	0.422	0.197	0.544	0.544
0.367	0.628	0.299	0.388	0.188	0.531	0.532
0.309	0.611	0.296	0.387	0.159	0.526	0.469
0.309	0.535	0.276	0.350	0.155	0.484	0.422
0.301	0.532	0.269	0.327	0.150	0.458	0.375
0.299	0.512	0.261	0.322	0.150	0.405	0.364
0.282	0.498	0.251	0.312	0.149	0.397	0.345
0.277	0.486	0.250	0.297	0.142	0.372	0.325
0.276	0.452	0.239	0.283	0.137	0.364	0.317
0.270	0.450	0.238	0.273	0.137	0.356	0.306
0.260	0.441	0.223	0.272	0.132	0.341	0.304
0.220	0.440	0.221	0.257	0.132	0.339	0.296
0.168	0.419	0.206	0.255	0.131	0.323	0.294
RCP4.5, 2080s						
Observed	csiro-mk3	bcc-csm1-1	gfdl-esmsg	ipsl-cm5a-ir	micro-esm-chem	mpi-esm-ir
1.033	1.836	1.125	1.714	0.374	1.861	1.522
0.759	1.270	0.977	1.247	0.351	1.528	1.413
0.728	1.227	0.844	1.076	0.350	1.274	0.986
0.690	1.198	0.822	0.946	0.341	0.941	0.744
0.472	1.063	0.711	0.926	0.283	0.808	0.695
0.471	0.984	0.540	0.732	0.239	0.693	0.695
0.387	0.852	0.538	0.703	0.233	0.691	0.686
0.368	0.768	0.508	0.529	0.216	0.622	0.605
0.367	0.720	0.469	0.502	0.203	0.621	0.535
0.309	0.716	0.462	0.441	0.182	0.615	0.463
0.309	0.648	0.438	0.425	0.177	0.503	0.449
0.301	0.644	0.419	0.418	0.165	0.496	0.442
0.299	0.606	0.394	0.412	0.164	0.459	0.427
0.282	0.599	0.349	0.373	0.149	0.445	0.404
0.277	0.585	0.333	0.357	0.149	0.428	0.392

0.276	0.572	0.330	0.347	0.147	0.407	0.389
0.270	0.550	0.326	0.338	0.146	0.397	0.375
0.260	0.546	0.314	0.320	0.144	0.391	0.358
0.220	0.544	0.312	0.281	0.143	0.379	0.357
0.168	0.529	0.291	0.262	0.142	0.332	0.355
RCP8.5, 2050s						
Observed	csiro-mk3	bcc-csm1-1	gfdl-esmsg	ipsl-cm5a-ir	micro-esm-chem	mpi-esm-ir
1.033	1.425	0.795	1.182	0.238	1.394	1.833
0.759	1.033	0.785	0.920	0.238	1.264	1.361
0.728	0.990	0.625	0.796	0.231	1.261	1.080
0.690	0.853	0.560	0.729	0.228	1.148	0.963
0.472	0.720	0.472	0.700	0.213	0.726	0.840
0.471	0.613	0.414	0.619	0.183	0.678	0.695
0.387	0.578	0.383	0.600	0.161	0.616	0.679
0.368	0.537	0.351	0.483	0.161	0.576	0.677
0.367	0.526	0.339	0.408	0.153	0.545	0.664
0.309	0.516	0.332	0.365	0.129	0.534	0.655
0.309	0.508	0.293	0.342	0.127	0.528	0.535
0.301	0.462	0.269	0.333	0.127	0.484	0.513
0.299	0.447	0.263	0.325	0.126	0.439	0.501
0.282	0.446	0.255	0.315	0.126	0.419	0.499
0.277	0.434	0.251	0.293	0.116	0.376	0.489
0.276	0.429	0.247	0.292	0.107	0.356	0.447
0.270	0.424	0.243	0.270	0.107	0.356	0.439
0.260	0.424	0.241	0.266	0.106	0.346	0.412
0.220	0.410	0.235	0.246	0.106	0.321	0.409
0.168	0.393	0.227	0.228	0.105	0.307	
RCP8.5, 2080s						
Observed	csiro-mk3	bcc-csm1-1	gfdl-esmsg	ipsl-cm5a-ir	micro-esm-chem	mpi-esm-ir
1.033	1.824	0.928	1.149	0.213	1.523	1.983
0.759	1.229	0.874	0.901	0.213	1.053	1.424
0.728	1.206	0.753	0.793	0.198	1.004	1.007
0.690	1.205	0.718	0.751	0.193	0.938	0.975
0.472	1.043	0.585	0.739	0.191	0.716	0.886
0.471	0.917	0.499	0.646	0.173	0.588	0.781
0.387	0.901	0.495	0.596	0.146	0.585	0.766
0.368	0.814	0.404	0.486	0.141	0.557	0.759
0.367	0.792	0.381	0.393	0.134	0.449	0.583
0.309	0.763	0.377	0.383	0.125	0.434	0.541
0.309	0.716	0.356	0.337	0.117	0.434	0.534

0.301	0.668	0.339	0.333	0.116	0.405	
0.299	0.665	0.309	0.330	0.116	0.392	
0.282	0.664	0.291	0.320	0.113	0.387	
0.277	0.662	0.291	0.311	0.103	0.380	
0.276	0.546	0.286	0.286	0.094	0.355	
0.270	0.545	0.280	0.284	0.093	0.353	
0.260	0.526	0.266	0.274	0.089	0.351	
0.220	0.521	0.251	0.237	0.087	0.336	
0.168	0.515	0.244	0.235	0.087	0.324	

Downscaled Precipitation (mm/month)

RCP4.5, 2050s							
Month	Observed	bcc-csm1-1	csiro-mk3-6	gfdl-esm2g	ipsl-cm5a-lr	mpi-esm	miroc-esm-chem
J	60.778	77.000	58.250	77.583	153.000	68.000	83.833
F	62.297	89.083	59.833	85.250	104.500	56.833	89.500
M	102.912	124.167	98.750	121.750	175.000	107.417	81.917
A	124.962	179.667	165.750	143.417	272.167	137.250	122.667
M	93.700	127.917	86.500	81.833	182.000	70.583	68.917
J	38.293	37.000	30.250	36.917	29.417	30.083	29.667
J	34.664	32.833	31.750	39.917	34.250	37.333	31.417
A	70.435	53.667	59.250	64.250	85.917	75.667	67.083
S	120.266	140.083	84.583	106.750	121.583	109.167	94.250
O	149.579	167.917	95.000	154.583	224.417	105.500	78.583
N	145.016	218.583	144.417	211.083	304.333	163.750	123.667
D	96.785	102.667	76.500	122.667	185.500	105.500	94.833
	RCP4.5, 2080s						
Month	Observed	bcc-csm1-1	csiro-mk3-6	gfdl-esm2g	ipsl-cm5a-lr	mpi-esm	miroc-esm-chem
J	60.778	82.333	61.667	84.833	123.583	69.750	84.833
F	62.297	72.250	66.833	104.750	114.667	71.167	89.167
M	102.912	145.750	121.500	123.417	191.500	101.583	94.583
A	124.962	168.417	172.500	172.083	293.250	140.833	131.500
M	93.700	116.417	103.250	75.917	168.083	66.333	79.417
J	38.293	45.333	37.500	31.500	33.917	35.750	31.667
J	34.664	32.083	35.417	35.917	38.583	41.667	35.083
A	70.435	60.500	67.750	61.917	92.500	72.167	70.500

S	120.266	130.083	80.167	111.000	130.333	118.500	94.583
O	149.579	139.667	81.417	167.500	258.833	112.667	79.417
N	145.016	193.333	156.500	196.333	372.250	162.500	114.500
D	96.785	105.083	73.583	129.250	279.333	94.583	125.417
	RCP8.5, 2050s						
Month	Observed	bcc-csm1-1	csiro-mk3-6	gfdl-esm2g	ipsl-cm5a-lr	mpi-esm	miroc-esm-chem
J	60.778	67.167	64.833	85.500	164.500	57.000	85.000
F	62.297	97.167	77.833	95.167	108.333	67.083	71.000
M	102.912	136.667	108.417	130.667	184.833	108.500	85.250
A	124.962	185.083	157.917	169.167	299.833	142.667	131.750
M	93.700	116.250	89.750	53.917	226.583	66.500	76.417
J	38.293	40.833	34.667	31.167	37.750	27.500	30.500
J	34.664	33.667	35.250	35.083	37.333	36.667	32.417
A	70.435	51.917	76.250	63.917	84.667	66.417	65.333
S	120.266	142.333	82.500	106.500	122.333	97.500	105.750
O	149.579	172.833	78.167	153.250	261.250	104.833	84.667
N	145.016	188.750	138.250	233.167	354.917	152.583	124.500
D	96.785	79.917	82.417	125.917	262.833	101.667	126.500
	RCP8.5, 2080s						
Month	Observed	bcc-csm1-1	csiro-mk3-6	gfdl-esm2g	ipsl-cm5a-lr	mpi-esm	miroc-esm-chem
J	60.778	86.167	65.500	95.333	215.083	62.833	72.333
F	62.297	93.250	79.167	111.250	118.167	47.417	81.417
M	102.912	148.167	125.750	132.917	267.000	100.000	111.667
A	124.962	167.500	174.667	199.083	384.500	128.750	176.500
M	93.700	118.500	93.083	43.417	250.417	57.500	104.083
J	38.293	49.583	37.917	36.083	48.250	27.583	36.833
J	34.664	36.417	37.583	40.167	41.250	36.583	35.583
A	70.435	58.667	66.500	66.667	91.000	63.833	89.500
S	120.266	136.833	76.750	138.000	164.333	103.167	124.833
O	149.579	200.167	56.167	181.500	339.250	118.333	83.250
N	145.016	205.167	165.417	248.833	447.083	176.500	125.455
D	96.785	105.083	85.750	208.750	355.667	108.333	128.667

Downscaled T_{max} (°C)

RCP4.5, 2050s							
Month	Observed	bcc-csm1-1	csiro-mk3-6	gfdl-esm2g	ipsl-cm5a-lr	mpi-esm	miroc-esm-chem
J	27.212	27.767	29.008	27.058	27.467	27.008	27.675
F	27.235	27.658	29.467	26.758	28.458	27.750	28.133
M	27.156	28.042	29.433	26.342	28.175	27.258	28.167
A	26.795	26.383	27.667	26.208	26.858	26.125	27.092
M	26.784	26.592	28.017	26.642	26.992	26.783	26.742
J	26.731	27.383	28.575	26.750	27.492	27.183	26.883
J	27.629	28.042	28.742	27.342	28.358	27.425	27.342
A	27.432	28.600	28.767	27.567	28.425	27.142	27.650
S	28.141	28.000	28.383	27.667	28.192	26.692	27.475
O	28.030	27.208	28.175	27.283	27.650	26.650	27.333
N	27.271	26.325	27.392	26.442	27.317	25.883	26.925
D	26.548	26.583	27.958	26.225	27.517	26.250	26.925
RCP4.5, 2080s							
Month	Observed	bcc-csm1-1	csiro-mk3-6	gfdl-esm2g	ipsl-cm5a-lr	mpi-esm	miroc-esm-chem
J	27.212	28.083	29.908	27.442	28.850	27.525	28.017
F	27.235	28.258	30.067	26.058	28.983	27.767	28.467
M	27.156	28.233	30.108	26.433	28.600	27.867	28.658
A	26.795	26.783	28.067	26.167	27.225	26.408	27.600
M	26.784	26.767	28.300	26.850	27.617	27.217	27.325
J	26.731	27.383	29.067	26.975	28.033	27.425	27.383
J	27.629	28.325	29.225	27.617	28.800	27.558	27.700
A	27.432	28.717	29.200	27.708	29.125	27.492	27.708
S	28.141	28.167	29.142	27.717	28.683	27.133	27.900
O	28.030	27.542	29.100	27.267	27.783	26.733	27.650
N	27.271	26.808	27.858	26.550	27.675	26.067	27.275
D	26.548	26.825	28.617	26.483	28.208	26.667	26.975
RCP8.5, 2050s							
Month	Observed	bcc-csm1-1	csiro-mk3-6	gfdl-esm2g	ipsl-cm5a-lr	mpi-esm	miroc-esm-chem
J	27.212	28.867	29.225	28.783	28.783	28.683	28.267
F	27.235	28.492	29.658	28.408	29.492	29.067	28.675
M	27.156	28.633	29.925	28.150	28.750	29.250	29.067
A	26.795	27.575	27.875	27.583	27.267	28.017	27.842
M	26.784	27.292	27.633	28.183	27.608	28.408	27.592

J	26.731	28.150	28.958	27.808	28.108	28.517	27.633
J	27.629	28.983	28.933	28.475	28.825	28.708	28.133
A	27.432	29.525	28.608	28.625	29.125	28.892	28.600
S	28.141	29.058	28.558	28.567	28.592	28.550	27.925
O	28.030	27.833	28.542	28.042	28.383	28.417	28.183
N	27.271	27.433	27.950	26.967	27.750	27.850	27.600
D	26.548	27.775	28.050	27.225	28.275	27.908	27.442
RCP8.5, 2080s							
Months	Observed	bcc-csm1-1	csiro-mk3-6	gfdl-esm2g	ipsl-cm5a-lr	mpi-esm	miroc-esm-chem
J	27.212	29.800	31.217	29.700	30.842	30.333	30.133
F	27.235	29.950	31.067	28.508	31.333	30.983	30.400
M	27.156	29.800	31.442	28.867	30.408	31.000	30.542
A	26.795	28.592	29.483	28.583	29.117	29.892	29.267
M	26.784	28.667	30.425	29.275	29.458	30.817	29.600
J	26.731	29.483	31.042	29.300	30.008	30.758	29.900
J	27.629	30.267	30.992	29.650	30.533	30.458	31.392
A	27.432	31.167	30.575	30.325	30.867	31.242	30.417
S	28.141	30.517	30.475	30.175	30.225	30.375	30.158
O	28.030	29.233	30.242	29.475	29.717	29.942	29.892
N	27.271	28.550	29.058	28.167	29.925	28.933	29.442
D	26.548	29.167	29.725	28.283	30.017	29.025	29.075

Downscaled T_{min} (°C)

RCP4.5, 2050s							
Month	Observed	bcc-csm1-1	csiro-mk3-6	gfdl-esm2g	ipsl-cm5a-lr	mpi-esm	miroc-esm-chem
J	14.160	15.208	15.008	15.642	16.267	15.758	15.292
F	14.210	15.375	14.783	15.692	16.883	15.725	15.742
M	14.290	15.883	15.450	16.258	17.708	16.758	16.217
A	14.919	15.817	15.375	16.083	17.817	16.408	15.983
M	14.577	15.625	15.050	15.900	16.900	16.225	15.442
J	14.088	14.575	14.717	14.792	16.000	15.433	14.375
J	13.940	14.050	14.633	14.550	15.692	15.217	14.000
A	14.349	15.133	15.525	15.417	16.675	16.008	15.225
S	14.468	15.417	15.192	15.475	16.442	15.967	15.458
O	14.531	15.317	14.875	15.892	16.967	16.108	15.467
N	14.539	15.108	14.933	15.758	16.642	16.008	15.567
D	14.182	15.025	14.700	15.300	16.650	15.617	15.083

RCP4.5, 2080s							
Month	Observed	bcc-csm1-1	csiro-mk3-6	gfdl-esm2g	ipsl-cm5a-lr	mpi-esm	miroc-esm-chem
J	14.160	15.725	16.025	15.892	16.683	16.000	15.825
F	14.210	16.108	16.533	15.800	17.525	16.142	16.142
M	14.290	16.475	16.525	16.350	18.250	16.975	16.767
A	14.919	16.483	15.958	16.217	18.467	16.683	16.525
M	14.577	16.358	16.150	15.858	17.525	16.792	16.100
J	14.088	15.275	15.792	15.033	16.217	15.800	15.027
J	13.940	14.900	15.933	14.508	15.892	15.608	14.742
A	14.349	15.925	16.175	15.283	16.517	16.217	15.650
S	14.468	16.100	15.400	15.508	16.850	16.150	15.758
O	14.531	16.067	14.792	15.883	17.700	16.442	16.042
N	14.539	15.883	15.633	15.600	17.250	16.408	16.100
D	14.182	15.675	15.258	15.483	17.100	16.033	15.682
RCP8.5, 2050s							
Month	Observed	bcc-csm1-1	csiro-mk3-6	gfdl-esm2g	ipsl-cm5a-lr	mpi-esm	miroc-esm-chem
J	14.160	15.783	16.983	16.533	17.200	15.958	15.850
F	14.210	16.150	17.225	16.642	17.717	16.317	16.242
M	14.290	16.458	17.617	17.192	18.158	17.008	16.925
A	14.919	16.608	17.075	16.975	18.450	16.725	16.758
M	14.577	16.375	17.042	16.800	17.792	16.867	16.317
J	14.088	15.283	16.433	15.767	16.600	15.733	15.333
J	13.940	14.842	16.358	15.225	16.392	15.692	14.967
A	14.349	15.925	16.925	16.075	17.483	16.258	16.125
S	14.468	16.267	16.392	16.350	17.525	16.183	16.325
O	14.531	16.033	16.442	16.600	17.583	16.408	16.450
N	14.539	15.842	16.467	16.392	17.525	16.367	16.300
D	14.182	15.600	16.475	16.067	17.275	15.975	15.875
RCP8.5, 2080s							
Months	1960-1970	bcc-csm1-1	csiro-mk3-6	gfdl-esm2g	ipsl-cm5a-lr	mpi-esm	miroc-esm-chem
J	14.160	17.133	19.292	18.175	19.608	18.483	17.858
F	14.210	17.350	19.733	18.283	20.517	18.850	18.200
M	14.290	17.708	19.583	18.617	20.992	19.550	18.800
A	14.919	17.675	18.825	18.408	20.942	19.383	18.717
M	14.577	17.783	19.158	17.958	19.892	19.467	18.733
J	14.088	16.942	19.033	17.308	18.917	18.467	17.842
J	13.940	16.275	18.817	16.675	18.758	18.042	17.433
A	14.349	17.408	19.250	17.408	19.708	18.875	18.683

S	14.468	17.450	18.483	17.783	20.225	18.817	18.483
O	14.531	17.175	18.158	17.725	20.458	18.717	18.225
N	14.539	17.092	18.275	17.708	19.592	18.742	18.242
D	14.182	17.083	18.750	17.908	19.933	18.225	17.808